2007

# Biochemical Characterization of hTRF1 and hTEP1, Two Proteins Involved in Telomere Maintenance

Kambiz Tahmaseb
*Wright State University*

# Biochemical Characterization of hTRF1 and hTEP1, Two Proteins Involved in Telomere Maintenance

A dissertation submitted in partial fulfillment of the
requirements for the degree of
Doctor of Philosophy

By

Kambiz Tahmaseb
B.S., Willamette University, 1999

_____

2007
Wright State University

WRIGHT STATE UNIVERSITY

SCHOOL OF GRADUATE STUDIES

May 24, 2007

I HEREBY RECOMMEND THAT THE DISSERTATION PREPARED UNDER MY SUPERVISION BY Kambiz Tahmaseb ENTITLED Biochemical Characterization of hTRF1 and hTEP1, Two Proteins involved in Telomere Maintenance BE ACCEPTED IN PARTIAL FULFILLMENT OF THE REQUIREMENTS FOR THE DEGREE OF Doctor of Philosophy.

John J. Turchi, Ph.D.
Dissertation Director

Gerald M. Alter, Ph.D.
Director, Biomedical Sciences
Ph.D. Program

Joseph F. Thomas, Jr., Ph.D.
Dean, School of Graduate Studies

Committee on
Final Examination

John J. Turchi, Ph.D.

Mill W. Miller, Ph.D.

Michael Leffak, Ph.D.

Robert W. Putnam, Ph.D.

Gerald M. Alter, Ph.D.

ABSTRACT

Tahmaseb, Kambiz Ph.D., Biomedical Sciences Ph.D. Program, Wright State University, 2007. Biochemical Characterization of hTRF1 and hTEP1, Two Proteins Involved in Telomere Maintenance

Telomeres are the structures that protect the ends of linear chromosomes from fusion and degradation. The telomere consists of tandem repeated DNA sequences that can range from hundreds of bases to kilo-bases depending on the organism. As the cells of an organism replicate their DNA, these repeats are lost due to the end replication problem, where the ends of linear DNA cannot be fully replicated. As the telomeres are shortened through each round of replication, they eventually reach a critical point. Once the telomeres are too short and the cell risks losing coding sequences, a signaling pathway is initiated that causes the cell to senesce. However, cells that require continuous replication (i.e., stem cells, germ cells, and cancer cells) require constant maintenance of their telomeres in order to not enter senescence. The majority of these cells use the multimeric protein telomerase and a host of other proteins to maintain the lengths of their chromosomes. Eukaryotic telomerase is a nucleo-protein complex consisting of the telomerase RNA (TR), telomere end reverse transcriptase (TERT), and telomerase associated protein 1 (TEP1). Furthermore, telomeric length is regulated by a host of telomeric binding proteins.

This thesis focuses on two proteins important for human telomeric maintenance. The first is human TEP1 (hTEP1) which is a subunit of

telomerase. This large protein contains the RNA binding domain that binds hTR. Though the RNA binding subunit of hTEP1 has been partially purified before, full-length hTEP1 has been refractory to biochemical analysis due to the inability to express and purify this large protein. Here we reveal the very first purification of full-length hTEP1. Furthermore, where the RNA binding domain of hTEP1 alone does not show specific interaction with hTR, we show that full-length hTEP1 binds hTR specifically.

The second protein of interest in this thesis is the human telomeric repeat binding factor 1 (hTRF1). This protein is one of the telomeric binding proteins that plays a critical role in telomere structure and stability. hTRF1 is also important as a regulator of telomeric length. hTRF1 has been shown to bind telomeric DNA specifically and my data reveals details of this surprisingly complex interaction using a sensitive intrinsic fluorescence kinetic technique. Our results demonstrate that hTRF1 binds to both telomeric and non-telomeric DNA. However, hTRF1 exhibits different characteristics as it binds telomeric DNA and is able to distinguish between telomeric and non-telomeric tracts of DNA.

This new information on these two key players in the maintenance of telomeres will help us further understand how these complex DNA ends are preserved in the cell. Through this knowledge, we can devise better tests in understanding how immortal cell lines, such as cancer cells, function and proliferate, making it possible to identify novel therapeutic targets to inhibit this process.

TABLE OF CONTENTS

LIST OF FIGURES

LIST OF TABLES

# LIST OF ABBREVIATIONS

| | |
|---|---|
| AMV | avian myeloblastosis virus |
| BME | beta mercaptoethanol |
| bp | base pair(s) |
| BSA | bovine serum albumin |
| CPM | counts per minute |
| C-strand | cytosine rich strand |
| DEPC | diethyl pyrocarbonate |
| DNA | deoxyribonucleic acid |
| dNTP | deoxynucleoside triphosphates |
| DTT | dithiothreitol |
| *E. coli* | Escherichia coli |
| EDTA | ethylenediamine-tetraacetic acid |
| EGTA | ethylene glycol-bis(2-aminoethylether)-N,N,N',N'-tetraacetic acid |
| FBS | fetal bovine serum |
| G-strand | guanosine rich strand |
| h | human |
| HRP | horseradish peroxidase |
| MOI | multiplicity of infection |
| $NaP_i$ | sodium phosphate buffer |
| PBS | phosphate buffered saline |
| PCR | polymerase chain reaction |

| | |
|---|---|
| PEI | polyethylenimine |
| pfu | plaque forming unit |
| PKC | protein kinase C |
| Polα | polymerase alpha primase |
| POT | protector of telomeres |
| PP2A | protein phosphatase 2A |
| PVDF | polyvinylidene fluoride |
| RNA | ribonucleic acid |
| SDS | sodium dodecyl sulfate |
| SF | *Spodoptera frugiperda* |
| TBS | Tris-buffered saline |
| TE | Tris-EDTA |
| TEP | telomerase associated protein |
| TERT | telomerase end reverse transcriptase |
| TR | telomerase RNA |
| TRF | telomere repeat binding factor |

ACKNOWLEDGEMENT

The road to this point has been a fantastic adventure. Like any other adventure it has been full of action, plot twists, and most importantly full of wonderful and exciting characters. I am so thankful to all these individuals who made this story so interesting and successful. There are many whom I wish to acknowledge as I would never have gotten to this point without their help and input. One group that I owe gratitude to is my committee. I would like to thank Drs. Alter, Leffak, Miller, and Putnam for their input towards the development and successful closure of this project. I greatly appreciate your words of encouragement over the years, and your ability to challenge me mentally and scientifically.

In the BMB department I wish to thank Shannon Duncan and Cheryl Little for helping me over the years with my responsibilities as a student, and with getting me rooms and equipment for my talks and meetings. I would like to thank Dr. Organisciak for always having kind words for me, and for allowing me to finish my project in the old Turchi lab once everyone but me had moved out (and for sharing those fantastic cigars). I would like to thank Drs. Berberich, Leffak, and Kadakia for helping me with access to reagents and equipment while I was trying to finish my project at WSU. I would also like to thank Dr. Steve Patrick for allowing me to use his lab, cell culture room and supplies in order to finish my project.

The adventure would not have been dramatic without the presence of my many friends and co-workers while I worked at WSU. I would like to thank

Dannette Richards, La'Tonia Stiner, Jason Lehman, Jeff Horn, Brooke Andrews, Katie Pawelczak, Heather Fullenkamp, Dr. Pat Dennis, and Karen Henkels for all being wonderful friends and co-workers. I especially would like to thank my friend Kenneth Frey for being a great friend and colleague, and the catalyst behind many adventures. I would also have to give Diane Ponder special thanks for all the help over the years in the BMS office and with my pet birds.

One of the most wonderful outcomes of my tenure at Wright State University was the chance to meet my wife, Suzette Tahmaseb. I would not have finished my degree without her support. Her dedication, inspiration, and love have been the driving force that has led to my success.

I would like to thank my advisor, Dr. Turchi, for guiding me through this very difficult project. I will forever remember your words of wisdom, both in science and in life in general. I will always cherish the times I had in your lab. I also owe many of the complements I get during my current work to your teachings. Thank you for helping me to become a good - ethical scientist.

Lastly, I must thank my family. I would like to thank my brothers Kamran and Keyvan and their families. I would like to thank my sister Sepideh and her family for always thinking of me and remembering me. Most of all, I owe an infinite amount of gratitude to my parents Mr. Jafar and Mrs. Talat Tahmaseb. Not only did they give me life and raise me, but they made many sacrifices so that I could be a free man and able to pursue my dreams and happiness. I am so proud to have them as parents, and wish that I too could be as brave and selfless as they are. You are the true inspiration behind this adventure.

# DEDICATION

This work is dedicated to all those who dream. All those who dream of freedom and prosperity, who sacrifice all to achieve those basic human rights. This work is dedicated to the American Dream.

# I. BACKGROUND AND SIGNIFICANCE

## History:

Organisms containing linear chromosomes face numerous problems with maintaining their DNA length. Unprotected linear DNA may suffer fusion and degradation (reviewed in Blackburn & Szostak, 1984). The specific sequence of DNA, which protects chromosomal termini, is referred to as the telomere (telos, end; meros, part). Though the study of telomeres has been quite recent compared to other aspects of eukaryotic chromosomes, the study of chromosomal ends has been conducted for most of the last century. The term "telomere" was first coined by H. J. Muller (Muller, 1938). Muller studied rearrangements and breakage in the chromosomes of the insect *Drosophila melanogaster.* He observed that there is a "terminal gene" which "[has] a special function, that of sealing the end of the chromosome…and that for some reason a chromosome cannot persist indefinitely without having its ends thus sealed" (Muller, 1938). Further observations of the special features of the chromosomal ends came from the work of Barbara McClintock. Along with Muller, McClintock also observed that in maize plants, broken chromosomal termini have a tendency to fuse, which led to the formation of bridged chromosomes. These fused chromosomes would break during mitosis and result in different genotypes which in turn gave the phenotype of variegated kernels. She also observed that the "breakage-fusion-bridge cycle" ceased if the chromosome ends "healed",

which was a process not understood at the time (McClintock, 1939; McClintock, 1941; McClintock, 1942).

After the discovery of DNA's structure (Watson and Crick, 1953), the Russian scientist A.M. Olovnikov published the end replication problem theory (Olovnikov, 1971). Olovnikov realized that the ends of linear DNA cannot be blunt after replication. He theorized that there may be two overhangs due to incomplete replication by a DNA polymerase. In his theory, the polymerase would sit on the 3' end of the template strand, and the area at which it sits would not be synthesized, thus leading to a 3' end overhang. Furthermore, the polymerase would travel 5' to 3', but would not be able to synthesize the last several bases because it would fall off, thus leading to a 5' overhang. In both cases, the overhang is in the template strand. Though it was proven that the end replication problem does exist, his theory as to how the overhangs formed were later shown to be incorrect. However, Olovnikov theorized that the telomere (whose function was unknown at the time) might serve as a buffer for the sequences lost due to the end replication problem (Olovnikov, 1971) and this is now known to be accurate. One aspect of the end replication problem which Olovnikov did not consider was the RNA primer used in the synthesis of the lagging strand. It was J.D. Watson and his studies of T7 DNA who described the existence of 3' overhangs after replication (Watson, 1972). In this study Watson theorized that Okazaki fragments may cause incomplete replication of the lagging strand, though at the time it was not clear how Okazaki fragments were formed and processed.

The telomere field was stimulated by studies on the protists, specifically trypanosomes and *Tetrahymena*. Some of these protists are the cause of parasitic diseases such as malaria, and are of medical interest. They were also easy to cultivate and study, especially for the study of telomeres, because they have a tendency to carry fragmented chromosomes which in turn translates into many termini. In *Tetrahymena* it was discovered that these termini contain a tandem repeat sequence of dTTGGGG (Blackburn and Gall, 1978). In trypanosomes some of the active surface antigen genes lie at the telomeric ends so attention was focused on to the telomeres. It was demonstrated that the telomeres of these unicellular organisms go through length maintenance (Pays *et al*., 1983). This length maintenance was later explained by the discovery of the enzyme telomerase (Greider and Blackburn, 1985). The telomere field was then underway, and the sequence of the human telomere (Moyzis *et al*., 1988) and telomerase activity were demonstrated in human cells shortly after (Morin, 1989).

Telomere Structure:

As previously mentioned, the end replication problem causes telomeres to have overhangs at the 3' end (Figure 1). Through multiple cell divisions, the short 5' ends lead to shorter DNA molecules. If the DNA ends are not protected by telomeres, the organism will lose genes close to the termini (for reviews Blackburn & Szostak, 1984; Dandjinou *et al.,* 1999; Holt & Shay, 1999). The human telomere consists of the 5'd (TTAGGG) tandem repeats and can range from 2-15kbp (Moyzis *et al.,* 1988). Telomeres shorten through cell divisions

both in cell culture and in whole tissues (Harley *et al*., 1990; Hastie *et al*., 1990; Counter *et al*., 1992), and the rate is proportional to the length of the 3' overhang (Huffman *et al*., 2000). Once the protective telomere has become too short, the cell will stop dividing and irreversibly arrest in the $G_1$ phase of the cell cycle, also known as senescence.

The end replication problem, which leads to senescence, is thought to be a result of discontinuous replication of the lagging DNA strand. As the RNA primers of the Okazaki fragments are removed, the final primer at the 5' end is not replaced by DNA, making this strand shorter. However, *in vivo* observations have revealed that the 3' overhangs of chromosomes are 45 to 210 bp long (Makarov *et al*., 1997; McElligott & Wellinger, 1997; Wright *et al*., 1997) (instead of the shorter length of an RNA primer), and on average about 50 bp of telomeres are lost after each population doubling (Harley *et al*. 1990). Recent *in vitro* studies have demonstrated that the lagging strand is not primed and extended near the last 500 bp of the 3' complementary strand (Ohki et al., 2001). This *in vitro* observation supports the *in vivo* finding and suggests that the telomere shortening is the result of both the removal of the RNA primer from the 5' end and the inability of DNA primase to prime and synthesize at the ends of chromosomes. Furthermore, it is expected that replication of the original 5' strand will lead to a blunt ended DNA molecule due to continuous synthesis of the new 3' strand. However, it has been demonstrated that both yeast and mammalian cells maintain 3' overhangs on all chromosomes (Dionne & Wellinger 1996; Wellinger *et al.,* 1996; Makarov *et al*., 1997; Hemann & Greider,

1999). Therefore, blunt chromosome ends are processed to obtain 3' overhangs, suggesting that this structure is vital for cell function. Evidence also suggests that the overhangs are a result of 5' end degradation instead of 3' end elongation (Dionne & Wellinger 1996; Wellinger *et al*., 1996; McElligott & Wellinger, 1997).

Once these 3' overhangs are generated, one must consider how these ends are maintained. There are two theories as to how the overhangs are managed in the nucleus. The first theory is that they adopt a G-quartet structure. It has been demonstrated that DNA sequences with high guanosine content have a tendency to form base pairs between the guanosines (Henderson *et al*., 1987; Williamson, 1989). This G-G base pairing has the potential to form higher order structures such as hairpins, double hairpins, pseudoknots (Henderson *et al*., 1987), and G-quartets (Williamson, 1989). As the name implies, a G-quartet is a structure where four guanosines form hydrogen bonds in a square planar fashion. However, the G-quartet model has only been shown *in vitro* using protist telomeric DNA which is more G-rich than the mammalian counterpart. The mammalian telomeric repeat only forms G-quartets under non-physiological conditions such as high temperatures and/or low pH (Phan and Mergny, 2002).

The other theory for the maintenance of the telomeric overhangs is the t-loop model. The t-loop is formed when double-stranded telomeric DNA loops back upon itself, and the single-stranded 3' overhang becomes embedded within the double stranded telomeric tract (Griffith *et al*., 1999). The portion where the single stranded DNA is embedded in the double stranded region is known as the

D-loop. Recent *in vitro* experiments using electron microscopy have further supported the t-loop theory (Muñoz-Jordán *et al*., 2001; Stansel *et al*., 2001). The t-loop is facilitated and kept by the telomeric binding factor TRF2 (see next section for further details). Currently, the t-loop theory is the accepted model for mammalian telomere structure to maintain the end in a nonrecombinogenic state and protected from detection by DNA damage recognition proteins. This is demonstrated by the fact that cells, which have sufficient telomeres, may still senesce or apoptose once telomere end maintenance by the telomeric binding factors has been prohibited and hence the DNA end left exposed. Van Steensel *et al*. (1998) and Karlseder *et al*. (1999) demonstrated that the expression of the dominant negative mutant of TRF2 in immortalized cell lines induced senescence and apoptosis due to destabilization of the telomere ends from lack of binding by TRF2.

Telomeric Proteins and RNA:

In order to continue cell division, some cells activate the enzyme telomere terminal transferase (telomerase) (for review Liu, 1999) which extends the telomeric 3' end *de novo*. Telomerase was first isolated from the protist *Tetrahymena* (Greider & Blackburn, 1985) and later its activity was demonstrated in humans (Morin, 1989). Telomerase is specific for telomeric repeats. The mammalian telomerase recognizes and extends the single stranded $d(TTAGGG)_n$ 3' end of chromosomes. Due to the guanine content of the telomeric 5'-3' strand, it is referred to as the G-strand and inversely the 3'-5' strand is known as the C-strand. Telomerase is a cellular reverse transcriptase

which uses an intrinsic RNA template termed hTR (human telomerase RNA) to extend telomeric DNA. The two known protein components are the catalytic subunit (TERT) and another associated subunit of unclear function (TEP1) which we studied further and describe the findings in this thesis.

The telomerase catalytic subunit is known as the telomere end reverse transcriptase (TERT). Most human cells do not express the TERT subunit, resulting in no telomerase activity (Meyerson *et al*., 1997; Nakamura *et al*., 1997). hTERT was cloned by two labs simultaneously and was found to be composed of over 1100 amino acids with an estimated size of 127 kDa (Meyerson *et al*., 1997; Nakamura *et al*., 1997). The introduction of hTERT into telomerase negative cells leads to longer telomeres and increased replicative potential (Bodnar *et al*., 1998; Counter et al., 1998a). Conversely, the induction of a dominant-negative mutant of hTERT in telomerase positive cancer and immortalized cell lines leads to a decrease in telomere length and increased cell death (Zhang *et al*., 1999).

The structure of telomerase and regulation of telomerase activity remains to be fully elucidated. It has also been demonstrated that telomerase is a phosphoprotein, and PKC$\alpha$ is involved in the phosphorylation of telomerase (Li *et al*., 1998). It is known that inhibition of protein kinase C (PKC) (Ku *et al*., 1997) as well as *in vitro* addition of protein phosphatase 2A (PP2A) (Li *et al*., 1997) inhibit telomerase activity. Furthermore, any deletions in both the C and N-termini (outside of the catalytic domain) of hTERT completely diminish any enzymatic activity (Bachand and Autexier, 2001). It is not known whether these

termini are required for phosphorylation of hTERT, but they are not required for binding the telomeric RNA template molecule (hTR) (Bachand and Autexier, 2001). However, it is known that the deletion of amino acids 301-538 in the N-terminus and amino acids 914-928 in the C-terminus do keep hTERT from oligomerizing and inhibit telomerase activity. These mutants also have the ability to serve as dominant negatives, indicating that hTERT is most likely a dimer (Arai *et al*., 2002). It is also known that the C-terminus of hTERT is essential for telomerase maintenance. Though catalytically active, a tag on the hTERT C-terminus can keep telomerase from maintaining the telomeres of an immortalized cell line (Counter *et al*., 1998b; Ouellette *et al*., 1999).

The RNA molecule that hTERT uses as a template to synthesize telomeric repeats *de novo* is called hTR (Feng *et al*., 1995). hTR and hTERT are sufficient for telomerase activity *in vitro* (Masutomi *et al*., 2000). Telomerase deficient mice created by deletion of mTR gene are shown to suffer from genetic instability and shorter life span (Blasco *et al*., 1997; Rudolph *et al*., 1999). Mutations in hTR lead to defects in cells which require continuous division (i.e. skin, gut, and bone-marrow) and leads to dyskeratosis congenita in humans (Vulliamy *et al*., 2001). Bone-marrow failure and abnormal skin pigmentation characterize this disorder. This evidence further supports the theory that continuously dividing cells require the protection of telomeres and telomerase to continue normal function.

hTR is a RNA molecule of roughly 450 bases in length and with a complex secondary structure (Chen *et al*., 2000) (Figure 2). In addition to containing the

telomeric template, the hTR molecule has conserved CR4-CR5, H/ACA box, CR7, and the pseudoknot domains (Chen *et al*., 2000). Different deletion mutations have demonstrated that the first 159 nucleotides of hTR are sufficient for binding hTERT but not sufficient to produce telomerase activity, which requires the sequences between nucleotides 276-424 as well (Bachand and Autexier, 2001). This study and others (Chen and Greider, 2003) demonstrate that the presence of the template sequence is not enough for telomerase activity and that the hTR secondary structure plays a major role as well.

The final known telomerase subunit and one of particular interest in this research is telomerase associated protein 1. Human TEP1 (hTEP1) was cloned and characterized by the Harrington lab, and was found to be 2629 amino acids long resulting in a protein of 240 kDa (Harrington *et al*., 1997). hTEP1 interacts specifically with hTR *in vivo* like hTERT, and this activity is conserved through multiple species (Harrington *et al*., 1997). In fact, hTEP1 shares one third of its length with the *Tetrahymena* p80, which is a telomeric subunit of *Tetrahymena*. It was this homology with p80 that led to the discovery of TEP1 in the mammalian system.

In addition to the RNA binding domain that hTEP1 shares with p80, mammalian TEP1 also contains a series of WD40 repeats, and a nucleotide binding domain (Figure 3). WD40 repeats have been shown in other proteins to be important for protein-protein interactions (reviewed in Neer *et al*., 1994). TEP1 knockout mice have been shown to have normal telomere ends and telomerase function (Liu *et al*., 2000), thus the authors generalize that TEP1 is

not important in telomere function and maintenance in mammals. However, mice have different telomere length maintenance and telomerase activity than that found in humans. Furthermore, it is highly unlikely that a protein would be conserved across species and kingdoms, but not serve a crucial role in cellular function. Part of this function may lie in the interaction of hTEP1 with a large cytoplasmic ribonucleoprotein known as the vault particle (Kickhoefer *et al*., 1999), although the reason for this interaction remains to be elucidated as the role of vault particles remains an unknown.

Though hTEP1 has been cloned, it has not been purified, which may be because of hTEP1's large size and instability in solution. Other than the research done in this dissertation, there has been one other published account of hTEP1 purification. In this purification scheme only the p80 homology domain of hTEP1 was partially purified (Poderycki *et al*., 2005). Though this domain did successfully bind hTR and vault RNA's *in vivo*, little specificity was detected during binding experiments *in vitro*. As it will be demonstrated in this dissertation, this lack of specificity *in vitro* is due to the absence of the other two thirds of the protein. I will show later that the full length hTEP1 does show specificity in binding hTR *in vitro*.

In addition to telomerase, there are other proteins involved in the maintenance of telomeres. Telomeric elongation and stability are maintained by the binding of telomeric repeat binding factors (for review Greider, 1996). Two known telomeric repeat binding factors in the mammalian system are telomeric repeat binding factors 1 and 2 (TRF1 and TRF2). Both of these proteins are

specific for double stranded telomeric DNA (Broccoli *et al*., 1997). TRF1 was first identified and characterized by the de Lange laboratory (Chong *et al*., 1995) and regulates the maintenance of telomeric length (for review Smith and de Lange, 1997). TRF1 has the ability to bind and bend telomeric DNA to an angle of approximately 120$^{o}$ which is thought to be important for telomeric maintenance (Bianchi *et al*., 1997). Binding of TRF1 to telomeric DNA is not cooperative, yet it is length dependent, with longer telomeric tracts increasing TRF1 binding *in vitro* using electrophoretic mobility shift assays (EMSA) (Zhong *et al*., 1992). This evidence supports the hypothesis that the shortening of telomeres results in less TRF1 binding.

The binding of TRF1 to telomeres negatively regulates their extension. Inversely, inhibition of TRF1 in telomerase positive cells leads to telomeres of increasing length (van Steensel and de Lange, 1997), however the exact mechanism of telomeric length regulation by TRF1 is unknown. *In vitro* experiments demonstrate that TRF1 and TRF2 are not capable of reducing telomerase expression levels (Smogorzewska *et al*., 2000). It has recently been shown that TRF1 directly interacts with POT1 (protector of telomeres 1), which is a single strand telomeric binding factor. The same study has demonstrated that TRF1 is responsible for POT1 loading onto single stranded telomeric ends, and that removal of TRF1 or the mutation of POT1 correlates with increased telomeric length. This study suggests that POT1 may be one factor involved in length regulation by TRF1 (Loayza and de Lange, 2003). Another pathway by

which hTRF1 may control telomere length is through the inhibition of C-strand synthesis, which is further described in the next section.

TRF2 has been demonstrated to be involved with stabilizing telomeric structures rather than regulation of telomeric length. Inhibition of TRF2 leads to loss of G-strand overhangs, covalent fusion of telomere termini, chromosomal fusion, and apoptosis (van Steensel *et al*., 1998; Karlseder *et al*., 1999). Stabilization of telomeres by TRF2 is thought to arise from its ability to stabilize the t-loop structure of telomeres (Figure 4).

Both TRF1 and 2 form homodimers and contain a Myb-like helix-turn-helix DNA binding domain in their carboxy end which is required for sequence-specific binding of telomeres (König *et al*., 1998). Studies have demonstrated that TRF1 and 2 have high specificity for the mammalian telomeric repeat sequences (Zhong *et al*., 1992; Broccoli *et al*., 1997; Krutilina *et al*., 2001). Though TRF1 and 2 share similarities in motifs and activity, they do not heterodimerize because the N-terminus required for dimerization in TRF1 is acidic and the N-terminus of TRF2 is basic (Broccoli *et al*., 1997). This supports the observation that these proteins have non-overlapping functions at telomeres.

As telomeres shorten, fewer telomeric binding factors may bind, which may lead to unstable telomeres (Smogorzewska *et al*., 2000). This instability translates into the exposure of the telomeric ends, which would normally be concealed in the t-loop, which in turn can be detected as damaged DNA and lead to cellular senescence. This theory is further supported by the observation that unstable telomeres form dicentric chromosomes (Karlseder *et al*., 1999).

This observation demonstrates that the exposed telomeric ends do not separate in mitosis due to fusion. Depletion of TRF2 activity by a dominant-negative mutant causes senescence via p53 and p16/RB pathways, which are the same pathways that cause senescence in normal cells (Smogorzewska and de Lange, 2002), providing more evidence that senescence from short telomeres is caused by a lack of binding by TRF's.

All of the previous biochemical work on TRF1 and 2 have been steady state measurements of their activities. The ability of TRF1 to regulate telomeric length makes it an ideal candidate to study biochemically in order to understand telomeric function better. Therefore, in the body of this work we will show pre-steady state kinetic studies on TRF1 and its interaction with DNA, further demonstrating that this interaction is much more complex than previously thought.

Cellular Implications of Telomeres, Coordinated Synthesis, and Significance:

As mentioned previously, the works of Muller (1938) and McClintock (1939; 1941; 1942) have demonstrated the importance of chromosome ends. Telomeres are important in the protection of chromosomes from degradation and fusion. Due to the end replication problem, telomeres shorten and upon reaching a critical length the host cell stops dividing. This halting of cellular division is known as senescence. Senescence may be caused by telomeric instability induced by the shortening of the telomere (Counter *et al*., 1992), though it may also be caused by oxidative stress and oncogene activation (for review Lundberg *et al*., 2000). Shortened telomeres are recognized as damaged

DNA since the ATM (ataxia telangiectasia mutated) and p53 pathways are activated (Vaziri *et al*., 1997). Both ATM and p53 are involved in damage recognition, induction of senescence, and apoptosis in damaged cells. Furthermore, deactivation of the p53/pRb pathways leads to cells which continue to divide until crisis is reached (cells in crisis continue cell division through the loss of telomeres and coding sequences of the genome) (Vaziri & Benchimol, 1999). This supports the hypothesis that shortened telomeres are recognized as damaged DNA, because the deactivation of the damage recognition proteins leads to cells that do not senesce.

In order for cells to have unlimited replicative potential without major chromosomal malfunction, they need to continuously elongate their telomeres, which is where the protein telomerase becomes involved. As mentioned previously, telomerase selectively extends telomeric G-strand *de novo*. Therefore, it is not surprising that most immortalized cell lines and tumor cells possess telomerase activity (Counter *et al*., 1992; Kim *et al*., 1994). Telomeres are very important in the study of many cancer types. Telomerase activity is crucial to the growth of tumor cells, because without it the telomeres would diminish and the cells would senesce or reach crisis. Therefore, it is important to understand how telomere length can be regulated.

However, telomerase is only part of the equation. Little is known about C-strand synthesis. Understanding the complete synthesis of telomeres is the only way to fully understand how telomere maintenance is regulated. There is some evidence that C-strand synthesis occurs with the aid of polymerase alpha

primase (Pol α). Studies done in our lab and others have demonstrated that Pol α is capable of priming and synthesizing telomeric tracts (Reveal et al., 1997; Nozawa et al., 2000). Since no other priming polymerase has been identified for telomere synthesis, it is most likely that Pol α is functioning in C-strand synthesis. Our lab has also demonstrated that TRF1 is capable of inhibiting Pol α's ability to function on telomeric tracts (Smucker and Turchi, 2001). This interaction may very well explain why TRF1 is a negative regulator of telomere length, unlike the current dogma that assumes TRF1 inhibits G-strand synthesis, which has not been recapitulated.

Due to the complexity of telomeres and telomerase, it is very important to biochemically understand the role and function of each component. In this work, I isolated and studied two important components of telomeric maintenance: hTRF1 and hTEP1. Both proteins were purified and studied. In the case of hTEP1, the purification scheme outlined in these pages is the first successful purification of the full length protein. For hTRF1, though it has been previously purified successfully, I will discuss the first pre-steady state kinetics performed on this protein. Overall, this work is one more step towards understanding how telomeres function, and eventually may lead to a significant leap into our general understanding of cancer.

**Figure 1.** Simple schematic of the end replication problem. The black lines represent the original strands and the red lines represent the newly synthesized strands, with the blue line representing the RNA primer of the Okazaki fragment. On the right side, the short 5' strand leads to the formation of a short 3' strand, and upon processing the original 5' end becomes even shorter than before.

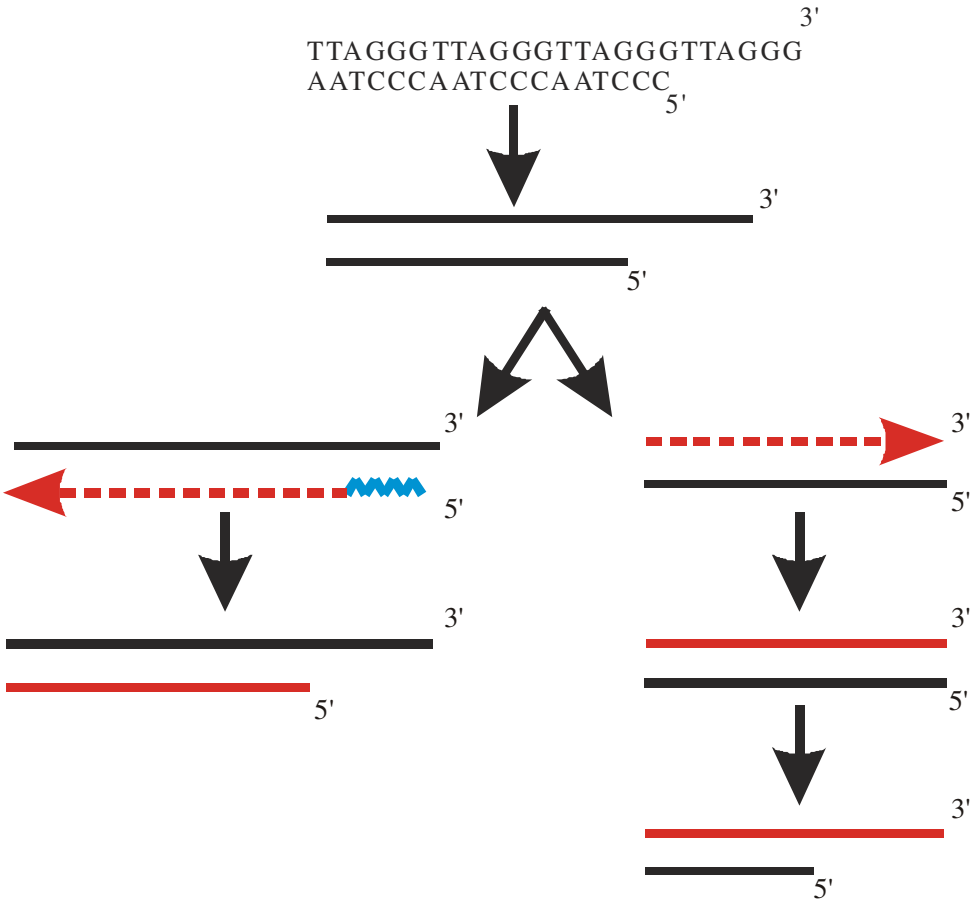
3'
TTAGGGTTAGGGTTAGGGTTAGGG
AATCCCAATCCCAATCCC
5'
3'
5'
3'
5'
3'
5'
3'
5'
3'
5'
3'
5'

**Figure 2.** The predicted secondary structure of hTR adapted from Bachand and Autexier, 2001. The box between bases 46 and 53 is the template region of hTR.

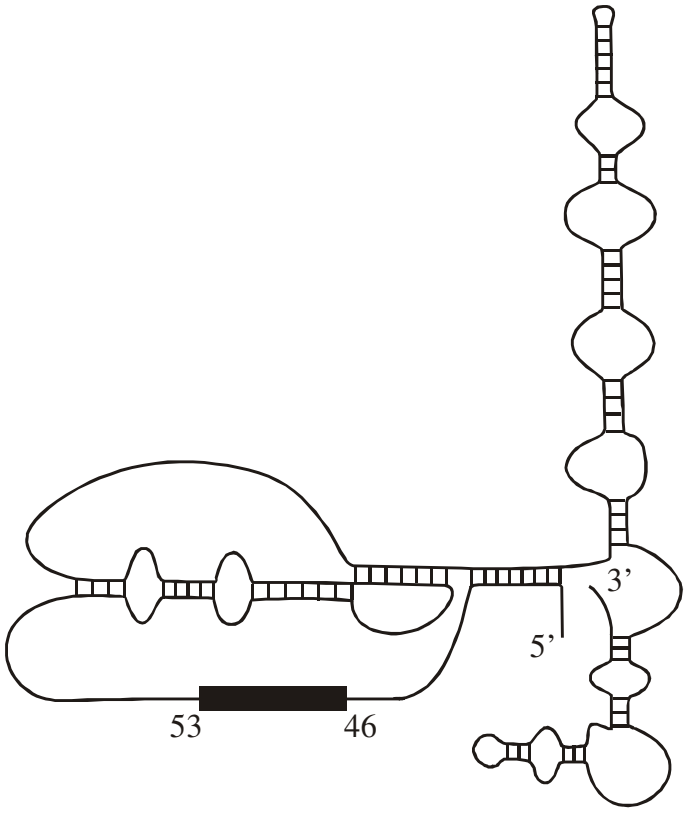
3'
5'
53
46

**Figure 3.** Schematic of the hTEP1 domains adapted from Harrington et al., 1997. a. The N-terminal repeats of hTEP1. b. The *Tetrahymena* p80 homology domain. c. The nucleotide binding domain. d. WD40 repeats.

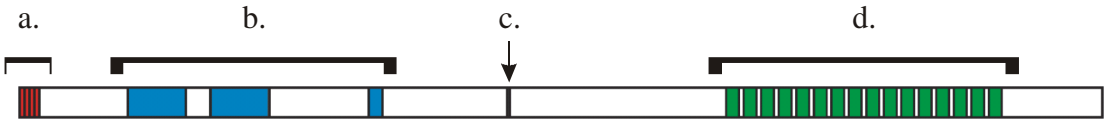
a.
b.
c.
d.

**Figure 4.** Schematic model of a telomeric t-loop. The blue proteins represent TRF1 and the red represent TRF2. The loop formed in the immediate vicinity of the infiltrating 3' end is the D-loop and is supported by TRF2.

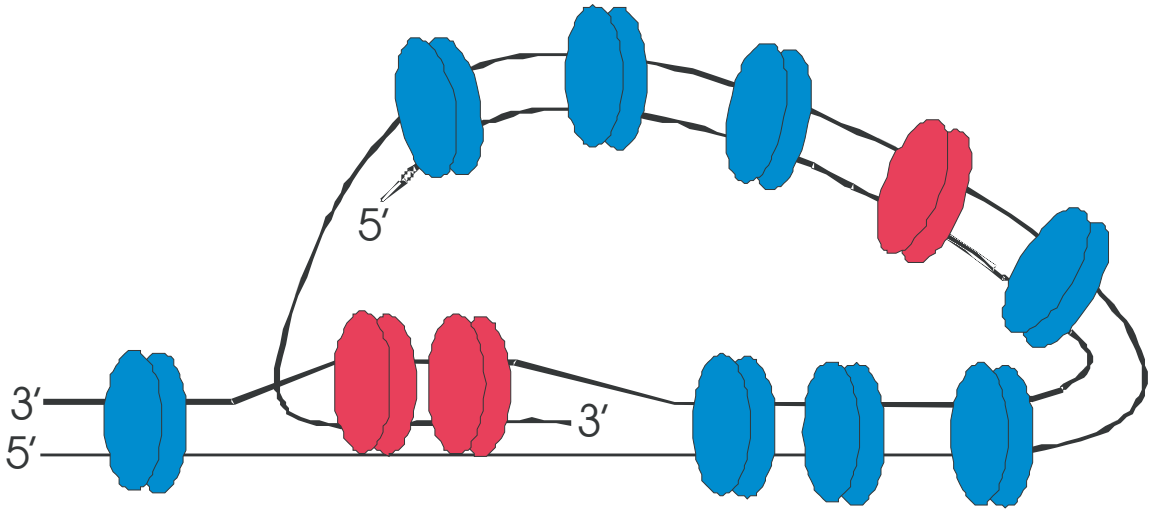
5′
3′
5′
3′

## II. MATERIALS AND METHODS

Cloning:

*hTR*: Whole cell RNA was extracted using the TRIzol® reagent (Invitrogen, Carlsbad, CA) and the instructions provided with the reagent. Briefly, confluent 293-S cells grown in a monolayer in a 35 mm dish were lysed by adding 1 ml of TRIzol® reagent. The solution was pipetted up and down to facilitate lysis. The solution was allowed to sit at room temperature for 5 minutes. 200 µl of chloroform was added to the lysis solution and shaken by hand to allow mixing. The solution was then centrifuged at 10,000 X g in a table-top centrifuge for 10 minutes at 4°C. The upper aqueous phase containing the RNA was removed and mixed with 0.5 ml of isopropanol. This solution was incubated in room temperature for 10 minutes and subsequently centrifuged as previously stated. The resulting pellet was washed using 1ml of 70% ethanol and re-centrifuged at 6000 X g for 5 minutes at 4°C. The pellet was then air dried, and dissolved in DEPC treated water. Absorption spectrophotometry was used to quantify the amount of RNA; agarose gels were used to assess the quality.

To generate single-stranded cDNA, the cDNA Cycle® Kit (Invitrogen, Carlsbad, CA) was employed using the kit guidelines. Briefly, the whole cell RNA was thawed on ice and 5 µg was used in each reaction. Random primers were added to the RNA. The solution was heated to 65°C for 10 minutes to remove the RNA secondary structure. The mixture was cooled to room temperature to allow primer binding and final reagents provided by the kit were added to the RNA/primer mix. The reagents included RNase inhibitor, reverse

transcription buffer, dNTP's, sodium pyrophosphate, and AMV reverse transcriptase. Upon mixing the solution, it was incubated at 42°C for one hour for reverse transcription to occur. Then the reaction was stopped by incubating the solution at 95°C for 2 minutes and then placed on ice. Subsequently the solution was chloroform/phenol extracted and ethanol precipitated and resuspended in DEPC treated water.

To amplify the cDNA of hTR, polymerase chain reactions (PCR) were performed. For the PCR experiments, reactions were carried out using the FailSafe™ PCR System in 25 µl. The specifics of this reaction are given under the results section.

The hTR cDNA was cloned into the pCR®-Blunt II-TOPO® vector using the Zero Blunt® TOPO® PCR cloning kit (Invitrogen, Carlsbad, CA). This kit allows for the cloning of blunt-ended PCR products into the vector without the use of restriction enzymes. Following the directions of the kit, the newly formed plasmids were used to transform TOP10 *E. coli* (provided by the kit). The transformed cells were plated and incubated overnight at 37°C. After the incubation, five colonies were picked for further analysis. These colonies were grown in 5 ml of LB broth overnight at 37°C in a shaker. The next day, the cells in each tube were sedimented for one minute at 8,000 X g on a table top centrifuge and a miniprep was performed using the QIAprep Spin Miniprep Kit (Qiagen, Valencia, CA). The plasmid yield was quantified using absorbance at 260 nm. The plasmids were then digested with restriction enzymes to confirm that hTR was properly cloned. One of the plasmids was then chosen to be sent

for sequencing by Cleveland Genomics (Cleveland, OH). Upon confirmation of the correct sequence, hTR was excised out of the pCR®-Blunt II-TOPO® vector using SacI and EcoRI restriction enzymes for insertion into the plasmid pBS+ which was also digested with the same restriction enzymes. The digested plasmid and insert were gel-purified using a 1% low melting point agarose gel with 1.5 µg/ml crystal violet dye run in 1X TAE buffer (40 mM Tris-acetate, 40 mM acetic acid, and 40 mM EDTA, pH 8.5). Crystal violet allows for the visualization of the DNA bands directly without the use of UV light which can be very damaging to the DNA. The DNA bands of the right size were cut out of the gel and the DNA was extracted using the QIAquick Gel Extraction Kit (Qiagen, Valencia, CA).

hTR was ligated into pBS+ by adding 400 ng of gel purified hTR to 45 ng of gel purified pBS+. The ligation mix also included 1X ligation buffer (50 mM Tris-HCl, 10 mM $MgCl_2$, 1 mM ATP, 10 mM DTT, 25 µg/ml BSA, pH 7.5 at room temperature), and 400 units of T4 DNA ligase (New England Biolabs, Ipswich, MA), all brought up to 20 µl by the addition of sterile water. Each reaction was incubated at 16°C overnight. As a negative control, the double digested vector without an insert was ligated, and as a positive control the vector with a single cut was ligated. After the ligation reactions were completed, the reactions were stopped by the addition of 20 mM EDTA. Then TOP10 *E. coli* were transformed using 4 µl of each reaction mix and plated. The plates were incubated at 37°C overnight. The next day, hTR colonies were checked using a quick PCR method. In this method, each bacterial colony was touched with a sterile tip and

then touched to the bottom of a PCR tube. Once 10 colonies were sampled this way, the tubes were heated in a microwave oven for 3 minutes to lyse the bacteria. The PCR mix for hTR was added to each tube and the PCR reactions were carried out using the procedures noted in the results section. The PCR products were analyzed using an agarose gel to determine which colonies contained the hTR insert. The selected colonies were then grown in LB broth for a maxiprep using Qiagen Plasmid Maxi kit (Qiagen, Valencia, CA) to obtain a larger quantity of the pBS+-hTR plasmid. Further restriction digests were performed to confirm the formation of pBS+-hTR and that hTR is in the correct orientation in relation to the T7 promoter.

*hTEP1*: All cloning specifics for hTEP1 are presented in the results section.

*hTRF1:* The hTRF1 cDNA was amplified from the Human Full Length cDNA kit (Panomics, Redwood City, CA). The reaction mixture included 1X cDNA buffer, 50 pmol of hTRF1 sense primer (5'ACGGCTAGCATCGAGCCATTTAAC 3') and hTRF1 antisense primer (5' GATCTGCAGAGCTTTTACAAACAC 3'), and 1 µl of human hull length cDNA. This mixture was heated in the thermocycler for 2 minutes at 82$^{o}$C and then 2 µl of rTth polymerase (Applied Biosystems, Foster City, CA) was added. Upon the addition of rTth, the reaction was heated to 94$^{o}$C for 1 minute followed by 40 cycles of 94$^{o}$C for 30 seconds, 55$^{o}$C for 1 minute, and 68$^{o}$C for 1 minute and 30 seconds. The cycles were followed by a final elongation step at 68$^{o}$C for 10 minutes. The reaction tube was stored at 4$^{o}$C for further analysis by agarose gel

electrophoresis. Upon confirmation of a band at 1.6 kbp the PCR product was cloned into the pCR®-Blunt II-TOPO® vector as described earlier. The cloned hTRF1 was analyzed using restriction digests. Once it was confirmed that hTRF1 was present, it was cloned into the pRSET B vector (Invitrogen, Carlsbad, CA). The pRSET B vector was chosen because it includes the sequences for a poly-histidine tag (His-tag) and an XPress tag, 5' of the targeted cDNA. pCR®-Blunt II-TOPO®-hTRF1 and pRSET B were both treated with BamHI and PstI restriction enzymes and gel-purified as described above. The gel-purified products were ligated as previously described, creating His-tagged and XPress-tagged hTRF1. His-XPress-hTRF1 was then cloned into pBacPAK 8 for the creation of a baculovirus. For this process, His-Xpress-hTRF1 and pBacPAK 8 were treated with XbaI and KpnI, and the fragments were purified and ligated as stated earlier.

Cell Culture:

All proteins in this work were expressed in the SF9 (*Spodoptera frugiperda*) cell culture system. Frozen SF9 cells at $3X10^6$ cells/ml were thawed and plated on a 100 mm dish in Grace's insect cell culture media (1liter contains 45.72 g of powdered media, 350 mg of sodium bicarbonate, 20 ml of 50X yeastolate, 3.3 g of lactalbumin, 10 ml of 100X penicillin-streptomycin, and 2 ml of 50 mg/ml Gentamicin), supplemented with 20% FBS and grown at $28^oC$. After the first 2-3 days, the cells were fed using Grace's media with only 10% FBS. Upon becoming confluent, the cells were scraped off using a rubber policeman and split into two 150 mm plates. Once the two plates were confluent the cells

were scraped again and placed into a 250 ml spinner flask in 100 ml of media. Cells were grown until a concentration of $1X10^6$ cells/ml was reached, at which time they were split down to $2.5\text{-}5X10^5$ cells/ml depending on how quickly more cells were needed.

Baculovirus:

*Construction*: The BacPAK™ Baculovirus Expression System (Clontech, Mountain View, CA), was used to generate the baculoviruses needed for these projects. In brief, $1X10^6$ cells in 1-2 ml of media were plated on a 35 mm dish. Once all of the cells had attached (1-2 hours) the media was removed and cells were washed with basic media (no FBS). After the wash, cells were allowed to sit in 2 ml of basic media for 30 minutes. During this incubation, 500 ng of pBacPAK 8 with the desired cDNA insert was mixed with 5 µl of Bsu36I digested pBacPAK 6 (provided by the kit), and the final volume was adjusted to 96 µl using sterile water. 4 µl of Bacfectin (transfection reagent provided by the kit) was added to the mix and was allowed to incubate for 15 minutes at room temperature. Upon the completion of all incubation steps, the media was removed from the cells and 1.5 ml of fresh basic media was added to the cells. The DNA-Bacfectin mix was then dripped into the media of the cells while swirling the plate. The transfection was allowed to continue for 5 hours at room temperature, and then 1.5 ml of complete medium was added to the cells and the plate was incubated for 72 hours. After 72 hours the media, which included the primary virus, was removed from the cells and sterile filtered to remove any cells or debris.

*Plaque purification*: To generate plaque purified virus, a plaque assay was performed on the primary virus. First, a 1:10 serial dilution was performed 4 times using insect media, so that at the end there were five tubes; undiluted, $10^{-1}$, $10^{-2}$, $10^{-3}$, and $10^{-4}$. Then, SF9 cells were plated into the 6 wells of a 6- well dish (each well is the size of a 35 mm dish) at a concentration of $1X10^{6}$ cells per well. Once all cells had attached, the media was removed and 125 µl of each virus dilution was added to each cell layer, with 125 µl of media added to the last well as a negative control. The lid of the plate was placed back and wrapped with Parafilm to avoid evaporation of the small liquid amount inside. During the incubation, sterile 2% low melting point agarose (melted) was mixed with equal volume of Grace's insect cell media to make a 1% agarose solution and stored in a $42^{o}C$ water bath to prevent solidification. After the incubation of the cells, the virus was removed and 1.5 ml of the agarose solution was added to the cells and allowed to solidify. 1.5 ml of media was added to the top of the agarose plug and the plates were allowed to incubate for 5 days. After the 5 days, the media on top of the agarose plug was removed and 1ml of 0.03% neutral red dye (diluted in sterile 1X PBS) was added to the top. The neutral red was allowed to soak in for 1-2 hours, removed, and the plates were inverted and incubated in the dark overnight. The next day, plaques where the cells had died would appear as clear spots in a background of red. Five plaques were then chosen to be amplified as plaque purified virus. The plaques were picked using glass Pasteur pipettes and resuspended in 1 ml of media. The virus was allowed to diffuse out overnight, after which the tube was spun down at 8,000 X g on a table

top centrifuge to remove any floating agarose or debris. The resulting supernatant was termed the plaque purified primary virus. One 0.5 ml aliquot of this virus was placed in a cryogenic tube and stored in -80°C, and the rest was kept at 4°C in the dark.

*Plaque Assay*: The steps for the plaque assay are very similar to those of plaque purification with some minor adjustments. Since higher titers of virus are involved for the plaque assay, dilutions were made in the range of $10^{-3}$ to $10^{-8}$. Also instead of removal, the viral plaques were counted. In order to determine the titer, the following equation was followed:

Titer (pfu/ml) = (#of plaques X 8)/dilution factor

In these studies the number of plaques were multiplied by 8 because 125 µl of virus was used and we want to know the titer in ml (8 X 125 µl = 1 ml). The units of the titer represent plaque forming units (pfu) per milliliter of virus.

*Amplification*: For the amplification of the plaque purified virus, SF9 cells were plated on 35 mm dishes at a concentration of $5X10^5$ cells per dish. Once cells had attached to the plate, 100 µl of plaque purified virus was added to the media. The plates were incubated at 28°C for 5 days. Upon the completion of the incubation, the media was removed and sterile filtered. This aliquot of virus was called the secondary virus. The secondary virus was then titered using the plaque assay procedure. One 1 ml aliquot of this virus was placed in a cryogenic tube and stored in -80°C, and the rest was kept at 4°C in the dark. The cells from this amplification were lysed in SDS sample buffer, heated to 85°C, and processed for Western blot analysis (described later).

For the amplification of secondary virus, 50 ml suspension culture of SF9 cells was prepared in a 100 ml spinner flask. The suspension culture was seeded at $5X10^5$ cells/ml, and $5X10^4$ pfu/ml of secondary virus was added. The suspension culture was then allowed to spin for 5 days at room temperature. Upon the completion of the incubation, the cell suspension was poured into a sterile 50 ml conical tube and spun at 1000 X g for 20 minutes at $4^oC$. The resulting supernatant was called the tertiary virus and was poured into a new sterile 50 ml conical tube and the pellet was discarded. Five to ten 1ml aliquots were placed in cryogenic tubes and frozen at $^-80^oC$, and the rest was kept as a working stock at $4^oC$ in the dark. Quaternary virus was generated the same way as tertiary virus. However, the amplifications were not taken past the quaternary virus. If more virus was needed, earlier virus aliquots were thawed and amplified.

Protein Expression and Purification:

*hTEP1*: The purification of hTEP1 will be described in the results section.

*SF9*: An extract made from uninfected SF9 cells was purified exactly as the hTEP1 preparation to be used as negative control. The fractions collected after the Q-column were the same fraction numbers as those collected for hTEP1 after purification on the Q-column.

*hTRF1*: His-hTRF1 (provided by Titia de Lange, Rockefeller University, NY) and His-XPress-hTRF1 (see virus info above) were produced by infecting a 100 ml spinner culture of SF9 cells with the corresponding hTRF1 baculovirus at an MOI of 10. The infection was allowed to proceed for 48 hours, at which time

the cells were collected by sedimentation at 1000 X g. Cells were washed with cold 1X PBS three times and spun down at 1000 X g after each wash. The cell pellet was weighed and 10X cell pellet volume of buffer R + 5 mM imidazole (50 mM $NaP_i$ pH 7.4, 1M KCl, 0.2% Triton X-100, 7 mM BME, and 5 mM imidazole) was added. The cells were Dounce homogenized using pestle A, and sonicated 20 times at 4 pulses each. 0.1% PEI was added to this extract and stirred for 10 minutes on a stir plate in the cold box. The PEI precipitated extract was centrifuged at 11,000 X g in a Beckman JA20 rotor for 30 minutes at 4$^{o}$C. In the meantime, the Ni-NTA matrix (Qiagen, Valencia, CA) was equilibrated to the buffer R + 5 mM imidazole. After the centrifugation step, the crude extract was added to the Ni-NTA matrix and allowed to rotate for mixing over 30 minutes. The Ni-NTA and extract slurry was then poured into a column and the flow - through collected separately as the column was washed with 10 column volumes of buffer R + 5 mM imidazole. The bound protein was eluted using buffer R + 350 mM imidazole. Fractions were collected in 1 ml aliquots and each was tested for protein content using the Bradford dye reagent. Fractions containing protein were then analyzed by SDS gel electrophoresis to determine in which fractions hTRF1 was present. The fractions containing hTRF1 were then pooled and diluted in a buffer similar to buffer R but one that did not include any KCl or imidazole in order to bring the salt concentration down to 100 mM. The diluted protein was then loaded onto a 1 ml heparin-sepharose column equilibrated to the 100 mM KCl buffer. The protein was then eluted off of the column using a linear gradient taking the salt concentration from 100 mM to 1 M. Fractions were

collected in 1 ml aliquots and analyzed for the presence of hTRF1, in the case of His-XPress-hTRF1 immunoblotting was performed using the XPress antibody (described later). Fractions containing hTRF1 were dialyzed using the hTRF1 dialysis buffer (20 mM HEPES pH 7.5, 1 mM BME, 500 mM KCl, and 20% glycerol).

SDS polyacrylamide gels and Immunoblotting:

For all SDS gels, the Hoefer SE 260 Mini-Vertical Unit (GE Healthcare Life Sciences, Piscataway, NJ) was used. Cast gels were 10 cm by 10.5 cm and 1 mm thick.

*hTEP1*: Protein samples were heated at 85$^{o}$C for 10 minutes in the presence of SDS sample buffer (35 mM Tris-HCl pH 6.8, 5% glycerol, 1.7% SDS, 0.2% bromophenol blue, and 1 mM DTT). The heated samples were quickly centrifuged on a table top centrifuge, and then loaded onto a SDS polyacrylamide gel (4% stacker and 6% separating). The gel was run at 35 mA until the dye front had run off of the gel. The gel was then silver stained for visualization.

For the immunoblotting of hTEP1, the samples were run on SDS gels. The proteins were then transferred onto a polyvinylidene fluoride (PVDF) membrane (Millipore, Billerica, MA) using the TE 22 Mini Tank Transfer Unit (GE Healthcare Life Sciences, Piscataway, NJ). The transfer process was performed at 400 mA for three hours in CAPS buffer (10 mM 3-cyclohexylamino-1-propane sulfonic acid, 10% methanol, pH 10.5). The PVDF was then removed from the transfer cassette and placed in a hybridization tube in the presence of blocking

buffer (2% nonfat dry milk in TBS-Tween [20 mM Tris-HCl pH 7.5, 170 mM NaCl, and 0.5% Tween 20]). The PVDF membrane was blocked for 15 minutes at 37$^{o}$C while being rotated in a hybridization oven. After the blocking step, the blocking buffer was discarded and the anti-Myc antibody 9E10 clone (Sigma-Aldrich, St. Louis, MO) was diluted to a 1:5000 ratio in blocking buffer and added to the hybridization tube. The primary antibody was allowed to incubate with the membrane for one hour at 37$^{o}$C. The antibody was then decanted and the membrane was washed with TBS-Tween containing 0.2% nonfat dry milk three times at 5 minute intervals. After the washes, the secondary antibody of goat anti-mouse IgG conjugated HRP (Bio-Rad Laboratories, Hercules, CA) at a 1:3000 dilution was added to the membrane in the hybridization tube and allowed to incubate as with the primary antibody. The secondary antibody was also washed the same as the primary antibody. Once the last wash was discarded, the membrane was housed in the hybridization tube to keep it from drying out. In order to visualize the Western blot, a chemiluminescence reagent (25 mM luminol, 90 mM p-coumaric acid, 100 mM Tris-HCl pH 8.5, and 0.03% hydrogen peroxide in 10 ml water) was poured onto the membrane and allowed to sit for 1 minute before being decanted. The membrane was then either exposed to film for autoradiography or visualized by a Fuji LAS-3000 instrument able to detect and digitally record the image from the chemiluminescence.

*hTRF1*: All procedures were followed as with hTEP1 with the exception that an 8% separation gel was used. The transfer procedure was carried out for

one hour. The anti-XPress monoclonal antibody (Invitrogen, Carlsbad, CA) was used as the primary antibody at a 1:10,000 dilution.

*In Vitro* Transcription:

*In vitro* transcription was used to generate radiolabeled hTR and control RNA molecules for hTEP1 activity assays (described later). This reaction was optimized by creating the following mix: 0.1 unit pyrophosphatase (Sigma-Aldrich, St. Louis, MO), 14 mM $MgSO_4$, 1X T7 polymerase buffer (New England Biolabs, Ipswich, MA), 20 µM ATP, and 4 mM UTP, CTP and GTP, 10mM DTT, 20 units RNase inhibitor (Roche, Nutley, NJ), T7 RNA polymerase (New England Biolabs, Ipswich, MA), 250ng template DNA, and 30 µCi [α -$^{32}$P] ATP (PerkinElmer, Wellesley, MA). Template DNA was generated by digesting pBS+-hTR with SacI and the empty pBS+ plasmid with AflIII to facilitate run off transcription of hTR and pBS+ (negative control) RNA's. The digested DNA was then gel-purified as described before.

The *in vitro* transcription mix was incubated at 37$^{o}$C for 2 hours, and heat inactivated at 70$^{o}$C for 15 minutes. The reaction was placed on ice, 40 units of DNase I (Invitrogen, Carlsbad, CA) was added, and the reaction was incubated at 37$^{o}$C for 15 minutes. After this final incubation, the mixture was heat inactivated as before. The mixture was then cleaned using the RNeasy Mini Kit (Qiagen, Valencia, CA). A scintillation counter was used to measure total counts from each reaction.

Electromobility Shift Assay (EMSA):

Radiolabeled hTR and pBS+ RNA were prepared as described in the previous section. Each 16 µl reaction included 1X telomerase buffer (50 mM Tris-HCl pH 8.2, 1 mM $MgCl_2$, 2 mM EGTA, 1mM BME, 1 mM spermidine, and 0.1 mM spermine), 10 units RNase inhibitor, and 40,000 CPM of radiolabelled RNA. Because of the very low concentrations of hTEP1 protein, it was added up to volume limits. Some reactions were run in the presence of cold inhibitor, which was either 30 µg of tRNA or 40 µg yeast RNA (Sigma-Aldrich, St Louis, MO). Reactions were incubated on ice for 30 minutes and then 4 µl of 5X stop gel buffer (50% glycerol, 50 mM EDTA, and 0.5% bromophenol blue) was added to each tube. The samples were then run on a 4% native acrylamide gel at 150 volts.

Fluorometry:

hTRF1 fluorescence was measured using a Cary Eclipse Fluorescence spectrophotometer (Varian, Palo Alto, CA) in 400 µl reaction volumes in the presence of 1X pol-α buffer (10 mM Tris-HCl pH 7.5, 5 mM $MgCl_2$, and 7.5 mM DTT), and 100 nM hTRF1. Protein and DNA concentration were selected based on titration studies. Fluorescence emission scans and excitation scans were performed on hTRF1 to determine the optimum emission and excitation wavelengths. The optimum excitation wavelength was determined to be 277 nm and an optimum emission wavelength of 335 nm at a slit width of 10 nm (Figure 14). For fluorescence quenching studies, first the solution with buffer and 500 nM DNA was zeroed. Then 100 nM protein was added while the cuvette was inside the instrument and quickly mixed by pipetting up and down. A kinetic read

(0.2 seconds per read) was then initiated for 15 minutes. Quenching with each DNA substrate (see below) was repeated at least 3-times and the quenching data was then averaged and plotted using the SigmaPlot software (Systat, Point Richmond, CA).

*DNA substrates*: The DNA substrates used for the kinetic studies of hTRF1 are listed in Table 1. Each strand was synthesized by Integrated DNA Technologies (Coralville, IA), and was then gel-purified using a 3 mm thick denaturing polyacrylamide gel. UV shadowing was used to visualize the DNA band and to remove that piece of the gel. The piece was then sheared using a 1 ml syringe and eluted overnight in 3-4 ml elution buffer (300 mM NaOAc, 1 mM EDTA, and 0.1% SDS) at 4$^{o}$C while rotating to mix. The eluted DNA was then removed from the gel pieces by filtration though a syringe filter (2 μm pore size), then was ethanol precipitated by adding 3 equal volumes of 100% ethanol, placing in the freezer for a minimum of 30 minutes, and sedimenting at 11,000 X g in a Beckman JA20 rotor for 1 hour at 4$^{o}$C. Each DNA pellet was then resuspended using TE buffer and the concentration was measured using absorbance at 260 nm. Double stranded DNA was generated by mixing equal concentrations of complementary strands with annealing buffer (50 mM Tris-HCl pH 7.5, 10 mM magnesium acetate, and 5 mM DTT), heating to 95$^{o}$C for 5 minutes, and cooling slowly to room temperature overnight.

**Table 1.** DNA substrates used for hTRF1 fluorescence quenching. Telomeric sequences are represented in bold lettering**.**

| Name | Sequence (5'-3') | Length |
|---|---|---|
| PS38.1 | ATCGCCTGAGTCAGAGCTAGCTAGCCCAGGATCCACCG | 38 |
| PS38.2 | CGGTGGATCCTGGGCTAGCTAGCTCTGACTCAGGCGAT | 38 |
| KT5.1 | ATCGCCTGAG**TTAGGGTTAGGGTTAGGG**GGATCCACCG | 38 |
| KT5.2 | CGGTGGATCC**CCCTAACCCTAACCCTAA**CTCAGGCGAT | 38 |
| KT5.3 | ATCGCCTGAG**TTAGGGTTAGGGTTAGGGTTAGGG**GGATCCACCG | 44 |
| KT5.4 | CGGTGGATCC**CCCTAACCCTAACCCTAACCCTAA**CTCAGGCGAT | 44 |
| JT20.2 | **CCCTAACCCTAACCCTAACCCTAA**TGGCTTCAGCATCCTG | 40 |
| JT20.3 | CAGGATGCTGAAGCCA**TTAGGGTTAGGGTTAGGGTTAGGG** | 40 |
| JT20.4 | **CCCTAACCCTAA**TGGCTTCAGCATCCTG | 28 |
| JT20.5 | CAGGATGCTGAAGCCA**TTAGGGTTAGGGTTAGGG** | 34 |
| JT20.6 | **CCCTAACCCTAACCCTAA**TGGCTTCAGCATCCTG | 34 |

# III. RESULTS

hTEP1:

The cDNA for Myc-tagged hTEP1 was generously provided by Lea Harrington (Ontario Cancer Institute-Amgen Institute, Toronto, Canada). The Myc-hTEP1 cDNA was placed into the pBacPAK8 plasmid (Clontech, Mountain View, CA) for the creation of the hTEP1 baculovirus. Due to the very large size of the insert (about 8 kbp), it was not possible to find two unique restriction enzymes for generating overhangs. Therefore, hTEP1 was cut with a restriction enzyme that gave an overhang on one end and cut with a blunt cutting restriction enzyme at the other end, still allowing directionality in cloning. hTEP1 was cut using NotI and SnaBI and pBacPAK8 was cut using NotI and StuI. The fragments were gel-purified, ligated, and used to create the hTEP1 baculovirus (see Materials and Methods). The blunt end ligation of the SnaBI site on Myc-hTEP1 with the StuI site of the plasmid results in a loss of both restriction sites in the final product. The resulting plasmid was used to generate the hTEP1 primary baculovirus (see Materials and Methods).

Upon analysis of the Western blot of the cells from the secondary virus preparation, the virus with the best protein expression was chosen and re-amplified. Using the amplified virus, a multiplicity of infection (MOI) (refers to the number of virus particles per cell) titration study was performed to determine the best virus titer for maximal protein production. The experiments were performed in a 6-well plate, where in the first well no virus was added, then an MOI of 0.5,

1, 5, 10, and 20 were added respectively. The infection was allowed to proceed for 48 hours and the cells were then lysed in SDS sample buffer for analysis via Western blots. The MOI that resulted in the largest band of Myc-hTEP1 was used for further amplifications of hTEP1. The MOI titrations of the Myc-hTEP1 baculovirus demonstrated that an MOI of 5 or 10 is optimal for the hTEP1 production. In fact, once the MOI was increased up to 20, there was a noted decrease in protein expression (Figure 5a). Although the MOI of 10 has a slight advantage to MOI of 5 in protein expression, due to the difficulties in amplifying the Myc-hTEP1 baculovirus, the MOI of 5 was used for subsequent large scale protein expressions.

Upon determining the optimal MOI, a time course study was conducted to determine maximal protein expression over time. The test was performed very similarly to the MOI study, except that infected wells were infected with the same MOI of virus. Samples were taken at 24 hour intervals by removing the media from the cells and lysing the cells in SDS sample buffer. Each sample was frozen at $^{-}80^{o}C$ until the final sample was taken, and then all samples were analyzed using immunoblotting. The infection time that resulted in the brightest Myc-hTEP1 band in the Western blot was used for all infections for the amplification of hTEP1. The time course studies demonstrated that the 48 hour incubation with the virus is optimal (Figure 5b). In fact, a large drop in protein levels were observed once the virus was incubated for a longer period (Figure 5b). This loss of either the Myc-tag or degradation of hTEP1 became a major issue in the purification of hTEP1, which will be addressed later.

For the purification of hTEP1, three buffers were made: buffer A - no salt buffer (20 mM HEPES pH 7.8, 0.5 mM EDTA, 0.5 mM EGTA, 1 mM DTT, 0.1% NP40, and 10% glycerol); buffer B - 1M NaCl buffer (buffer A plus 1 M NaCl); and dialysis buffer (20 mM HEPES, 0.5 mM EDTA, 0.5 mM EGTA, 100mM KCl, 1 mM BME, and 20% glycerol). All purification steps were carried out by mixing buffer A and B in proportions to give the desired salt concentration. At each step 1 mg/ml of E64, Pepstatin, Leupeptin, and PMSF (all from Sigma-Aldrich, St. Louis, MO) were added to the buffers.

200 ml of a SF9 cell suspension was infected with Myc-hTEP1 baculovirus at an MOI of 5. After 24 hours, 1 mg/ml of the cysteine-protease inhibitor E64 was added to the cells, as this significantly reduced the degradation of hTEP1 before the lysis step. The cells were then incubated for another 24 hours as determined by the time course study. After 48 hours, the cells were spun down at 1000 X g for 10 minutes in a Beckman JA10 rotor. The media was discarded and the cell pellet was resuspended in cold 1X PBS. The washed cell pellet was weighed and extraction buffer (90% buffer A and 10% buffer B) was added up to seven times the weight of the pellet and was used to resuspend the pellet. The cells were allowed to sit on ice for 10 minutes with extraction buffer. Then the cells were Dounce homogenized using pestle A for 20 times, sonicated 10 times at 4 pulses each, and finally Dounce homogenized 5 times. The extract was then poured into a 15 ml glass centrifuge tube and centrifuged at 11,000 X g in a Beckman JA20 rotor for 45 minutes or until the turbidity of the extract was

low (at 4$^{o}$C). The crude extract obtained was decanted and the volume measured.

One problem that we encountered during the extraction process was the inability to obtain all of the Myc-hTEP1 from the cells in the first extraction (Figure 6a). Therefore, in order to increase the hTEP1 yield, the cell pellet from the previous step was resuspended in half the volume of extraction buffer as previously used. The extraction process was repeated and the new extract was cleared.

Another problem that we encountered was the loss of the ability to detect Myc-hTEP1 using immunoblotting after Myc-hTEP1 had been extracted (Figure 6b). Detection by immunoblotting became imperative because full length hTEP1 was produced in very low levels and was therefore difficult to detect using SDS gels alone. The detectable amounts of Myc-hTEP1 would decrease on an hourly basis, with significant decreases in a 24 hour period even if sample was stored at -80$^{o}$C (Figure 6b). The loss of hTEP1 was partly solved by adding E64 to the cells prior to extraction (data not shown). Cysteine-proteases are expressed upon infection of SF9 cells and thus by adding the inhibitor 24 hours prior to extraction, much of the intracellular degradation of the over-expressed protein can be reduced (Hom and Volkman, 1998; Marensen and Justesen, 2001). The second step to reduce degradation was the ammonium sulfate precipitation of the crude extracts. hTEP1 was precipitated out of solution by the addition of 25% ammonium sulfate (Figure 7). The precipitation was carried out by adding solid ammonium sulfate (Sigma-Aldrich, St. Louis, MO) slowly (over 30 minutes)

up to 25% of total volume while stirring on ice. The mixture was then allowed to stir on ice for another 30 minutes to allow for all of the ammonium sulfate to go into solution. Then the precipitated protein was sedimented at 11,000 X g in a Beckman JA20 rotor for 30 minutes. The supernatant was discarded, and the pellet was resuspended in the same volume of extraction buffer as the cells were first resuspended in. This suspension was also sonicated one time for 10 pulses to break apart any leftover pelleted protein, and was then centrifuged at 1000 X g for 10 minutes to remove any insoluble protein. Finally the resolublized protein was dialyzed overnight in 100 mM salt buffer at 4$^{o}$C. The Myc-hTEP1 resuspended from the 25% ammonium sulfate cut remained stable in solution for up to one month (data not shown).

The more stable Myc-hTEP1 was then run on a 10 ml quaternary amine column (Q-column) equilibrated to 100 mM salt buffer, using a Biologic DuoFlow FPLC system (Bio-Rad Laboratories, Hercules, CA). The flow-through was collected separately, followed by five column volumes of wash. Then the protein was eluted using a linear gradient from 100 mM NaCl to 1 M NaCl collected in 1 ml fractions. 20 µl of each fraction was mixed with 140 µl of water and 40 µl of Bradford dye reagent (Bio-Rad Laboratories, Hercules, CA) each in a well of a 96-well clear plate. The presence of protein was qualitatively measured by reading the plate at 595 nm. The absorbance was plotted to visualize the relative fractions where protein is present. The fractions that included the proteins from the third peak of elution, which contained hTEP1, were collected and dialyzed overnight against the dialysis buffer (described above) (Figure 8a).

The final protein was run on a 6% SDS polyacrylamide gel for visualization of the protein through silver staining and Western blotting (Figure 8 b and c). Due to the very low expression of hTEP1, it was not possible to purify the protein further as it would become too dilute for detection. However, this is the first time full length hTEP1 has been purified to this level.

To determine the activity of the Myc-hTEP1, electromobility shift assays (EMSA) were employed. Radiolabeled hTR (substrate) and pBS+ RNA (negative control) were prepared for this assay. To obtain hTR for this purpose we obtained the hTR cDNA from 293-S cells (see Materials and Methods). Upon generating the cDNA library, it was amplified using PCR. For the PCR experiments, the primers KT3.1 (5' TATAAGCCGACTCGCCCG 3') and KT3.2 (5' GCATGTGTGAGCCGAGTC 3') were used (Figure 9a). These optimal primers were designed using the Vector NTI software (Invitrogen, Carlsbad, CA). The PCR reactions were carried using the FailSafe™ PCR System (Epicentre Biotechnologies, Madison, WI). The FailSafe™ PCR System is a PCR optimization kit, which comes with a mix of thermostable polymerases which includes both high fidelity and low fidelity polymerases. The kit also comes with a set of twelve different PCR buffers (labeled A-L), each including dNTP's and different amounts of magnesium chloride for optimization of the reaction. For the hTR PCR, 1 µM of each primer, 1 µl of cDNA, 1 unit of the enzyme mix were added to enough water to make twelve 12.5 µl solutions, and 12.5 µl of each PCR buffer was added to its corresponding tube to make a 25 µl final solution. Each tube was gently mixed and placed into the thermocycler. The cycling

program involved an initial 98°C denaturation step for 2 minutes, followed by 30 cycles of 98°C for 30 seconds, 55°C for 30 seconds, and 72°C for 45 seconds. The tubes were then placed in 4°C until further analysis. The analysis involved running 2 µl of each reaction on a 1% agarose gel. Reactions that had a band around the 500 bp mark were chosen for further analysis (Figure 9b). PCR products were digested with XbaI and PvuII restriction enzymes. PCR products that responded as expected to these digests were chosen for further cloning.

The hTR cDNA was placed downstream of the T7 promoter in the pBS+ plasmid to generate pBS+-hTR (see materials and methods) for the production of hTR, and pBS+ alone was used to generate the negative control RNA. *In vitro* run off transcription was used to generate hTR and pBS+ control RNA (materials and methods).

For most of the EMSA experiments, the ammonium sulfate cut of hTEP1 was used due to the higher concentration of the protein. In these EMSA experiments hTEP1 had a clear specificity for hTR and not for the pBS+ RNA (Figure 10). The binding of hTEP1 with hTR was quite strong, even in the presence of yeast total RNA (Figure 11, lane 4). However, this interaction could be disturbed by using whole cell RNA from a human cancer cell line (Figure 11, lane 5), which could be attributed to endogenous hTR molecules. Furthermore, the hTEP1/hTR band on the gel could not be super-shifted using the anti-Myc antibody (Figure 11, lane 3), though this is not surprising since the hTEP1-hTR complex is so large that the addition of an antibody will not make a difference in the total size and cause a supershift.

Since hTEP1 could not be purified fully, it was important to test whether the hTR binding observed was not due to a SF9 protein contaminant. Therefore, uninfected SF9 cells were harvested, and protein was purified as with hTEP1. The same fractions as those obtained in the hTEP1 preparation were collected and used in EMSA experiments (Figure 12, lanes 2-5). We did not observe any hTR specific binding, since most RNA binding activity could be competed in presence of competitor RNA (Figure 12, lanes 2-5). However, even though the hTEP1 concentrations were very low after the collection of the Q-column fractions (80 µg/ml total protein), we could still observe binding to hTR (Figure 12, lanes 14 and 17). This binding was also observed when the ammonium sulfate cut, was run on a SEC250 size exclusion column (Figure 12, lanes 18 and 19), though this hTEP1 prep is not as pure as the Q-column fractions. When using the higher concentration ammonium sulfate cuts, we did not observe any super-shift with the Myc antibody (Figure 11, lane 3). However, with the more pure fractions of hTEP1, even though we did not see a super-shift when the antibody was added, we saw more clear binding of hTR in the presence of the Myc antibody and more of the protein was pulled out of the well (Figure 12, lane 17).

In summary, I have successfully expressed and purified full length hTEP1 using the baculovirus expression system. The key to this purification was to quickly separate hTEP1 from other proteins that were degrading it. hTEP1 expressed in this manner has great affinity for hTR which was cloned and produced in quantities necessary to carry out these experiments.

hTRF1:

The hTRF1 cDNA was successfully cloned out of a total human cDNA library using polymerase chain reaction (see Materials and Methods). The cDNA was then placed downstream of the His-tag and the XPress-tag of the pRSET plasmid, and the newly tagged sequence was then placed into BacPak 8 for the creation of the baculovirus (see Materials and Methods). Plaques were analyzed using immunoblotting with the anti-XPress antibody, and one plaque was chosen for the amplification of hTRF1 (see Materials and Methods). hTRF1 was expressed and purified successfully using the methods previously described (Figure 13). Off of the final heparin column, two peaks of protein were obtained. Both peaks contained a band at 66 kDa which may have corresponded with hTRF1 (Figure 13a). However, the immunoblot with the anti-XPress antibody indicated that the His-tagged hTRF1 was only present in the first protein peak (Figure 13b, lane 1). Furthermore, this was also the cleanest peak with only one other major protein band visible after silver staining the gel (Figure 13).

*Fluorescence studies*: Intrinsic fluorescence was chosen as the main detection tool for hTRF1 interaction with telomeric DNA. Intrinsic fluorescence is an attractive tool, because it is a very direct and simple way to measure pre-steady state kinetics of protein activity. To determine if intrinsic protein fluorescence could be used, excitation and emission spectra were taken over the ranges expected for tryptophan fluorescence. The excitation wavelength of hTRF1 was found to be 283 nm and emission at 335 nm, typical of tryptophan

excitation and emission (Figure 14). This fluorescence was also quenched upon binding of telomeric DNA (Figure 15 and Table 1) and was not quenched upon incubation with non-telomeric DNA (Figure 15 and Table 1) in equilibrium readings (Figure 16). This interaction was also quite stable even as salt was titrated into the mix, as there was no observable change in fluorescence quenching even at 300 mM extra salt (Figure 16).

Upon establishing that hTRF1's fluorescence can be quenched in the presence of telomeric DNA, the next step was to make pre-steady state measurements of hTRF1 binding to telomeric DNA. Several different DNA substrates were chosen to complete this task (Table 1 and Figure 15). Substrates with 3-4 telomeric repeats were chosen based on early equilibrium DNA binding studies, which showed that three repeats are the minimum required to detect binding in an EMSA assay (Zhong et al. 1992). The first attempts at measuring the pre-steady state binding of hTRF1 to telomeric DNA was performed on a stopped flow instrument, which allows for measurement of intrinsic fluorescence quenching down to millisecond time points. Quenching of hTRF1 fluorescence could not be detected in the millisecond time range (data not shown). Upon increasing the measurement time to 10 seconds, the first fluorescence quenching of hTRF1 due to binding of DNA could be measured (Figure 17). However, this quenching was observed regardless of the DNA substrate used. Yet EMSA experiments carried out in our lab and published by others indicated that hTRF1 binds telomeric DNA specifically. Furthermore the

equilibrium binding experiment shown in Figure 16 also confirmed that hTRF1 exhibits a higher affinity for telomeric DNA versus non-telomeric DNA.

Based on the observations highlighted above, hTRF1 fluorescence quenching was carried out in a fluorometer (see materials and methods), where the measurements could be carried out in minute time frames. Using the fluorometer, it was determined that the fluorescence quenching was surprisingly slow, taking fifteen minutes (Figures 18-23). As observed with the stopped flow measurements, there is a drop in fluorescence for the first two minutes regardless of substrate used (Figures 18-23). However, after two minutes, there is a distinct difference between DNA with and without telomeric tracts (Figure 18 compared to 19-23). The non-telomeric DNA exhibits a quenching for the first two minutes (Figure 18), but then there is no further fluorescence quenching. The telomeric substrates all exhibit further quenching after this first two minute window (Figures 19-23). Furthermore, the quenching data for hTRF1 binding to non-telomeric DNA fits only a single exponential decay curve (Figure 18), indicating a single event taking place (i.e. protein binding to DNA). The quenching data for all of the telomeric substrates except for one (KT5.3+KT5.4, Figure 20) fit a double exponential decay curve (Figures 19,21-23), indicating that two events are taking place. One of these events is the binding of the DNA molecule as observed with non-telomeric DNA. It is theorized that the second event may very likely be a conformational change that allows hTRF1 to more fully bind telomeric DNA, and this process is quite slow. However further studies are required to fully understand what is taking place and what the true rates are.

One curious aspect of this study is that the substrate with four internal telomeric repeats (KT5.3+KT5.4) had fluorescent quenching that fit a single exponential decay curve (Figure 20). Nevertheless, the quenching observed is still stronger than that with the non-telomeric substrate.

Even though there is a very apparent difference between non-telomeric DNA and telomeric DNA, there is not a very large difference between the binding of hTRF1 to the different telomeric substrates (Figure 24). hTRF1 does not discriminate between an internal telomeric repeat or an end repeat (Figure 19 a and b). hTRF1 also does not interact differently with blunt telomeric ends or one with an overhang (Figure 24a). The only major difference observed is between three internal repeats (KT5.1+KT5.2) and four internal repeats (KT5.3+KT5.4). This difference is due to, as mentioned earlier, KT5.3+KT5.4 being the only substrate that led to a decay that fit a single exponential curve. Part of the reason why not all of the curves fit perfectly is a spike in fluorescence right around the eight minute mark (Figure 20, 21 and 23). This spike cannot be a simple coincidence, since data was collected for each substrate at least three separate times if not more. Further evidence for this spike not being a random phenomenon is that in all three cases it is occurring around the same time frame. Since the exact cause of this spike is unknown further studies are needed to determine the reason for its occurrence.

In summary, here I have shown the first experiments elucidating how hTRF1 binds to DNA. The data clearly suggest that hTRF1 binds both telomeric and non-telomeric DNA, though binding to non-telomeric DNA is quite weak.

Although very slow, hTRF1 recognizes telomeric DNA and potentially goes through a conformational change that allows it to bind this DNA much more strongly. Further tests are needed to measure the exact dissociation constants for hTRF1 binding to telomeric and non-telomeric DNA substrates.

**Figure 5**. Immunoblots of Myc-hTEP1 expression optimization. a. MOI titration study where, lane 1 is the uninfected control. Lanes 2-6 represent MOI of 0.5, 1, 5, 10 and 20 respectively. b. Time course of infection study with the Myc-hTEP1 baculovirus. Lane 1 is the non-infected control. Lanes 2-6 are samples taken at 24, 48, 72, 96 and 120 hours respectively.

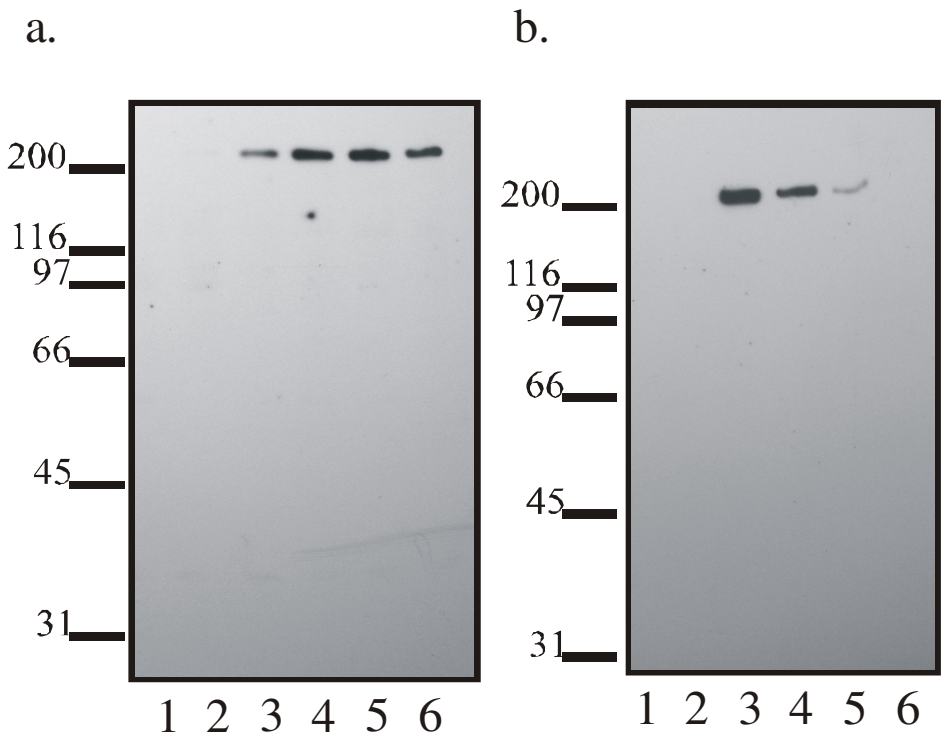
a.
b.
200
116
97
66
45
31
1 2 3 4 5 6
200
116
97
66
45
31
1 2 3 4 5 6

**Figure 6**. Immunoblots revealing Myc-hTEP1 degradation. a. Lane 1, cells were directly lysed in SDS sample buffer (materials and methods) and loaded onto the gel. Lane 2, first crude extract from cells. Lanes 3-4, re-extraction from the pellet formed after centrifugation of each extract. b. The immunoblot in each lane was performed on the same sample over 3 different days. Sample was saved at -80$^{o}$C over this time. After 48 hours the myc tag is completely lost.

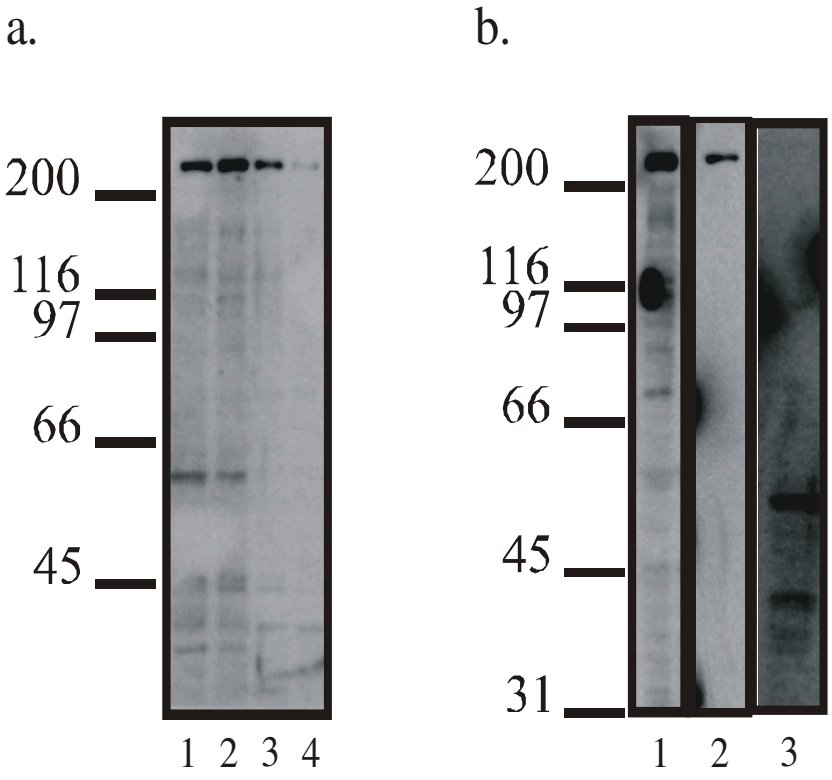
a.
200
116
97
66
45
1 2 3 4
b.
200
116
97
66
45
31
1 2 3

**Figure 7**. Immunoblot of Myc-hTEP1 after an ammonium sulfate precipitation. Lanes 2, 7 and 8 were left empty. Crude extract is present in lane 1. Lanes 3-6 are the supernatants from a 10%, 25%, 40%, and 60% ammonium sulfate precipitation respectively. Lanes 9-12 contain the pellets from the same precipitations shown in lanes 3-6. hTEP1 is present in the 25% pellet (lane 10).

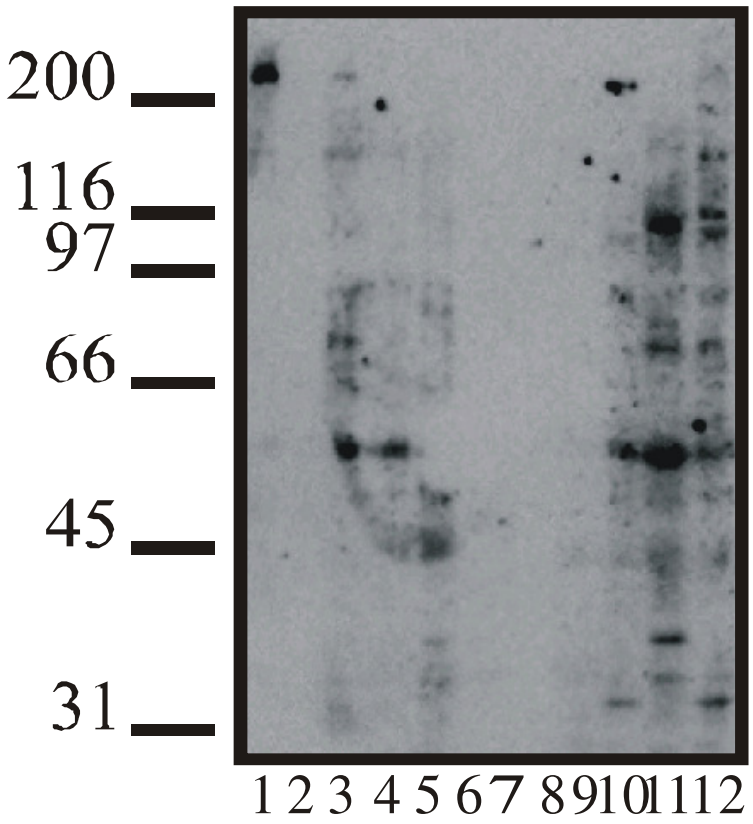
200
116
97
66
45
31
1 2 3 4 5 6 7 8 9 10 11 12

**Figure 8**. Purification of Myc-hTEP1. a. Chromatogram of Q-Sepharose fractionation of hTEP1. The graph represents protein as determined by a Bradford assay versus fraction number. Peak 1 is the flow through and bound proteins were eluted with a linear salt gradient. Peak 2 represents the first elution and does not contain hTEP1, and peak 3 represents hTEP1. b. Silver stained SDS gel of the protein obtained from the purification over the Q-column, Myc-hTEP1 is running at the 250kDa molecular weight standard. c. Western blot of the purified Myc-hTEP1.

a.

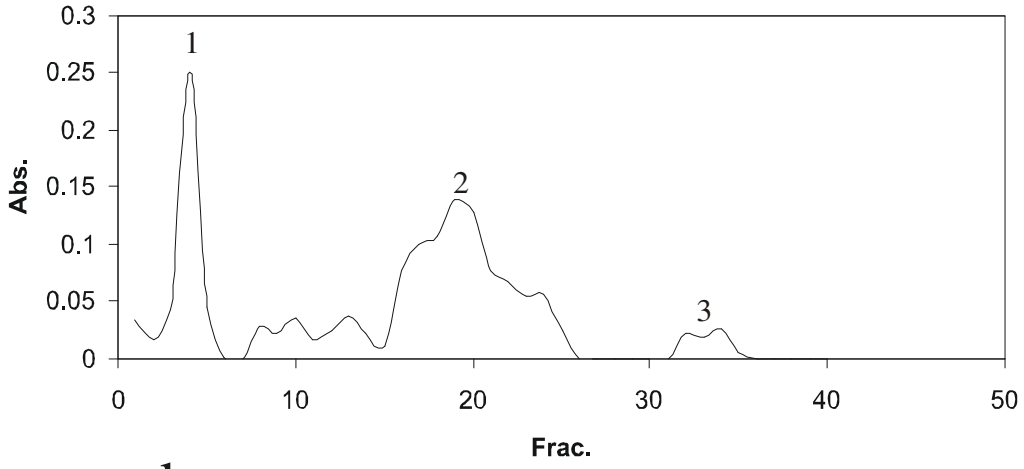
0.3
0.25
0.2
0.15
0.1
0.05
0
Abs.
1
2
3
0
10
20
30
40
50
Frac.

b.

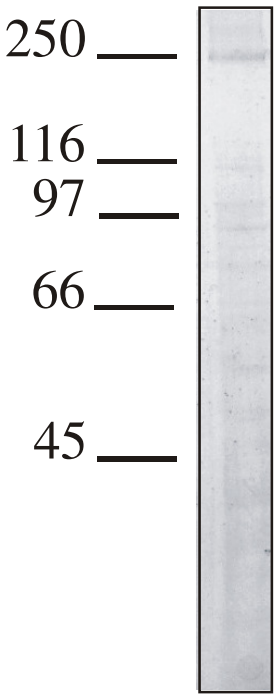
250
116
97
66
45

c.

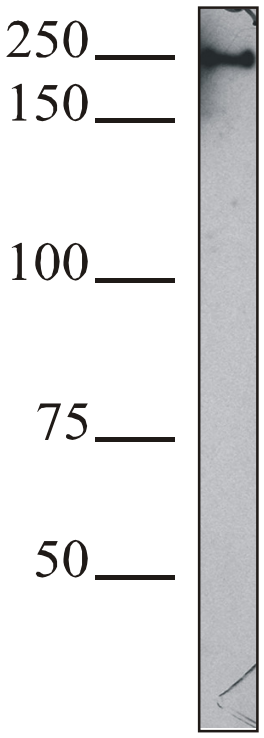
250
150
100
75
50

**Figure 9**. a. Cartoon of hTR cloning. Sense and antisense primers indicate the location of hTR on each plasmid. hTR was placed downstream of the T7 promoter and not the T3 promoter in the pBS+ plasmid. b. An agarose gel of the hTR cDNA PCR products. The product in the lane on the right was performed with the optimum amplification buffer described in Materials and Methods.

a.

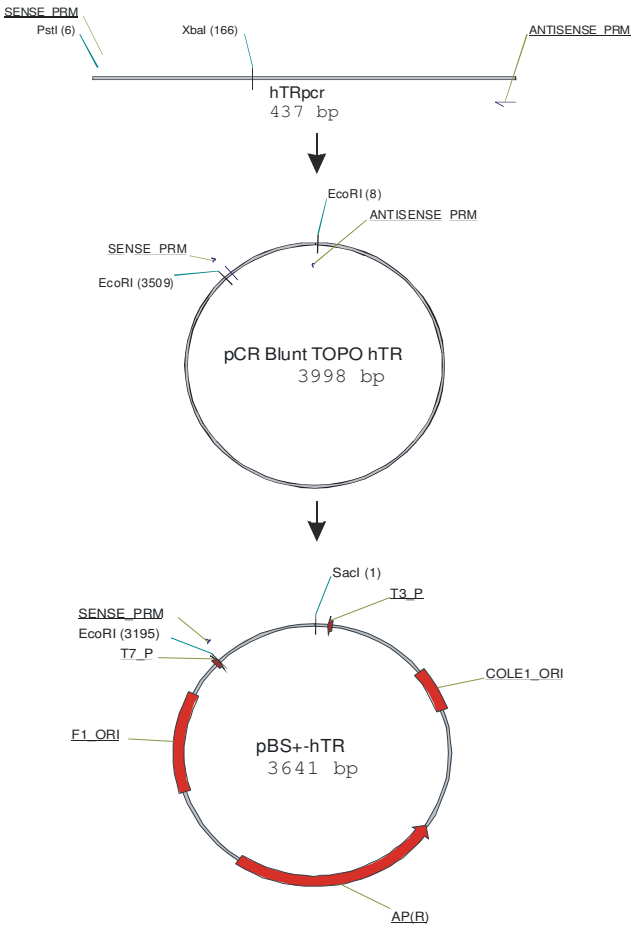
SENSE_PRM
PstI (6)
XbaI (166)
ANTISENSE_PRM
hTRpcr
437 bp
EcoRI (8)
ANTISENSE_PRM
SENSE_PRM
EcoRI (3509)
pCR Blunt TOPO hTR
3998 bp
SacI (1)
T3_P
SENSE_PRM
EcoRI (3195)
T7_P
COLE1_ORI
F1_ORI
pBS+-hTR
3641 bp
AP(R)

b.


600 bp
500 bp
400 bp

**Figure 10**. EMSA determining the activity and specificity of hTEP1 in presence of hTR and non-specific pBS+ RNA. Lanes 1-10 are in the presence of hTR and lanes 11-20 are in the presence of pBS+ RNA. Protein was titrated in lanes 2-5 and 12-15. tRNA was titrated in lanes 6-10 and 16-20. In the presence of the competitor the binding of hTEP1 to hTR is significantly enhanced (lanes 6-10) as non-specific binding by contaminating proteins is reduced. The reduction in binding of the pBS+ RNA in presence of cold competitor (lanes 16-20) reveals that full-length hTEP1 binds RNA molecules with specificity.

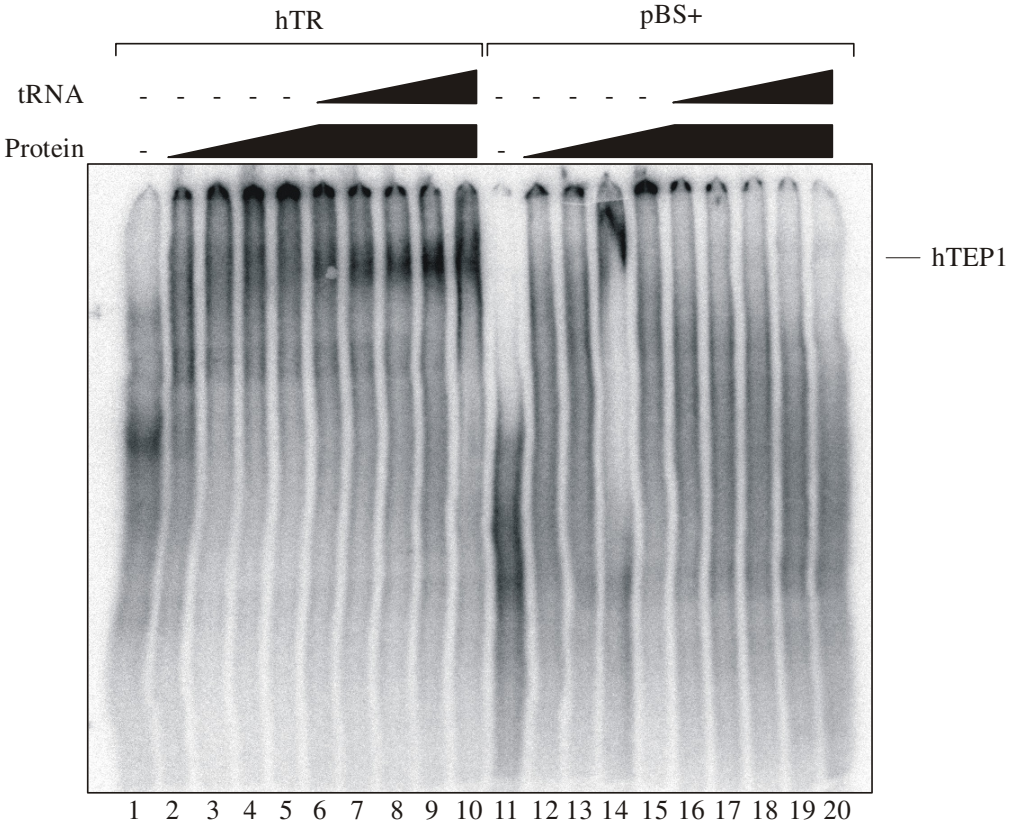
hTR
pBS+
tRNA
- - - - - - - - - - - -
Protein
- -
hTEP1
1 2 3 4 5 6 7 8 9 10 11 12 13 14 15 16 17 18 19 20

**Figure 11**. EMSA experiment determining the effect of different competitors and antibody on the binding of hTEP1 with hTR. Only total human cancer cell (H1299) RNA is capable of disrupting the hTEP1/hTR interaction.

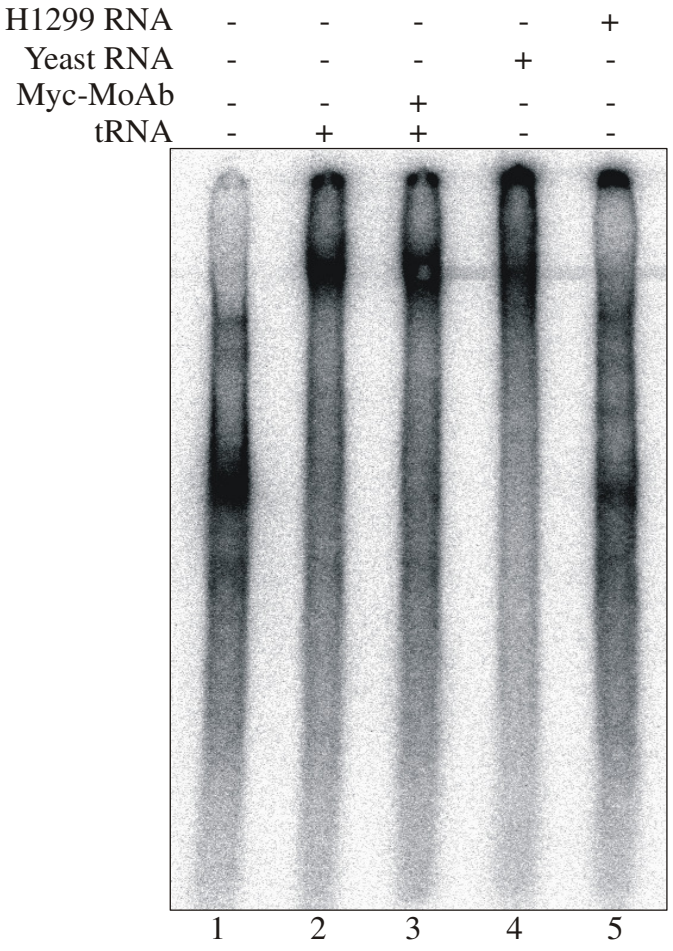
H1299 RNA - - - - +
Yeast RNA - - - + -
Myc-MoAb - - + - -
tRNA - + + - -
1 2 3 4 5

**Figure 12**. EMSA experiments comparing the mono-Q fractions of SF9 proteins (lanes 2-5), mono-Q purified hTEP1 (lanes 14 and 17) with Sec250 purified hTEP1 (lanes 18-19). All lanes have 800ng of protein, which was determined by the maximum volume of the Q-peak 2-hTEP1 that could be used. All lanes also contain 30 µg of tRNA unless stated otherwise. Q-peak 1 is the first peak of proteins that come off of the Q-column which does not contain any detectable hTEP1. Lanes 16 and 17 contain 1 µg of anti-Myc antibody (9E10), which can stabilize the hTEP1 binding to hTR (lane 17).

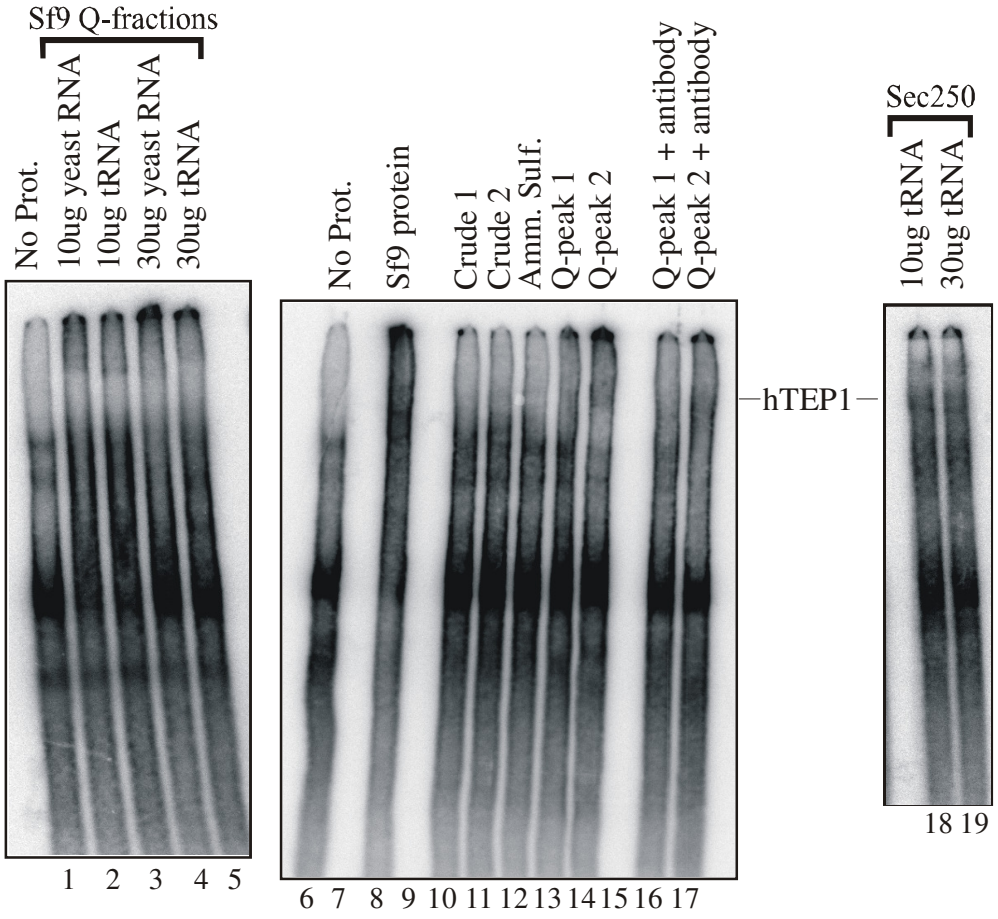
Sf9 Q-fractions
No Prot.
10ug yeast RNA
10ug tRNA
30ug yeast RNA
30ug tRNA
1 2 3 4 5
No Prot.
Sf9 protein
Crude 1
Crude 2
Amm. Sulf.
Q-peak 1
Q-peak 2
Q-peak 1 + antibody
Q-peak 2 + antibody
6 7 8 9 10 11 12 13 14 15 16 17
hTEP1
Sec250
10ug tRNA
30ug tRNA
18 19

**Figure 13**. His-Xpress-hTRF1 purification gel and Western blot. 1μg of protein is loaded into each well. a. Silver stained SDS gel of the two heparin protein pools. b. Immunoblot of the same samples represented in the silver stained gel. The immunoblot clearly demonstrates that hTRF1 is only present in the first protein peak that comes off of the heparin column (lane 1).

a.

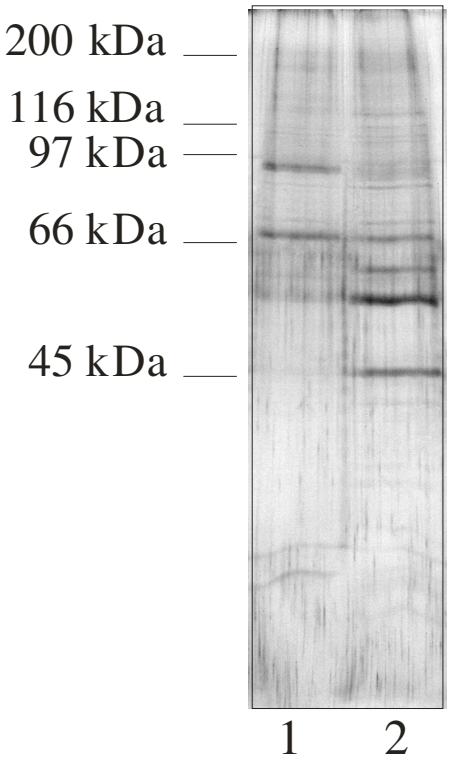
200 kDa
116 kDa
97 kDa
66 kDa
45 kDa
1
2

b.

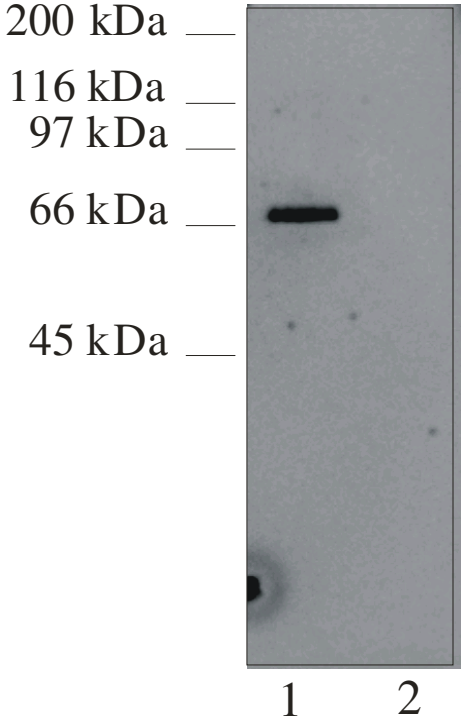
200 kDa
116 kDa
97 kDa
66 kDa
45 kDa
1
2

**Figure 14**. Excitation and emission spectra of hTRF1. a. Excitation spectrum of hTRF1 measuring emission at 340 nm. b. Emission spectrum of hTRF1 with excitation at 275 nm.

a.

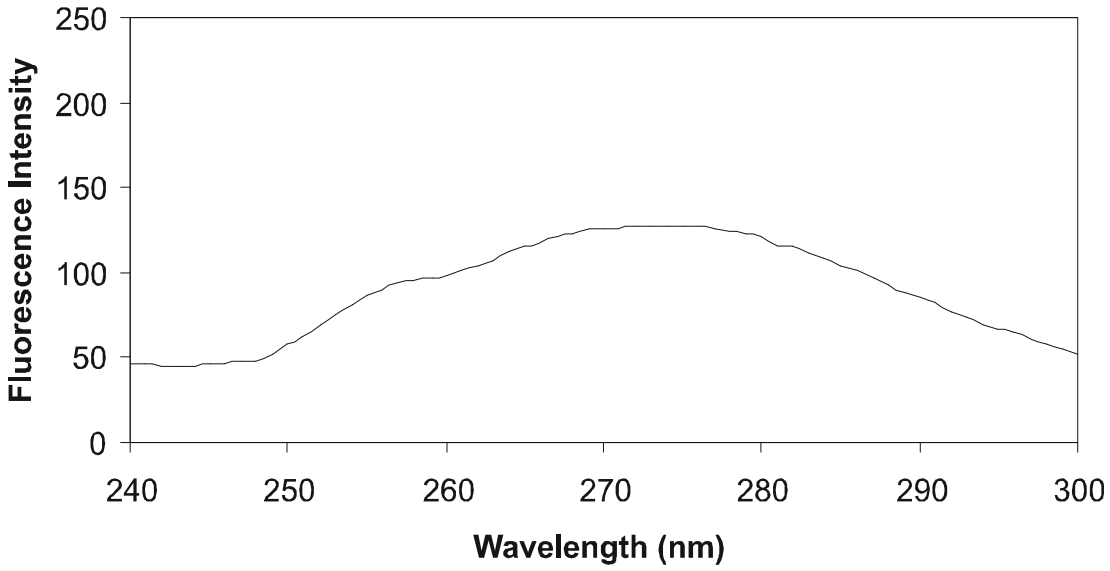
Fluorescence Intensity
250
200
150
100
50
0
240
250
260
270
280
290
300
Wavelength (nm)

b.

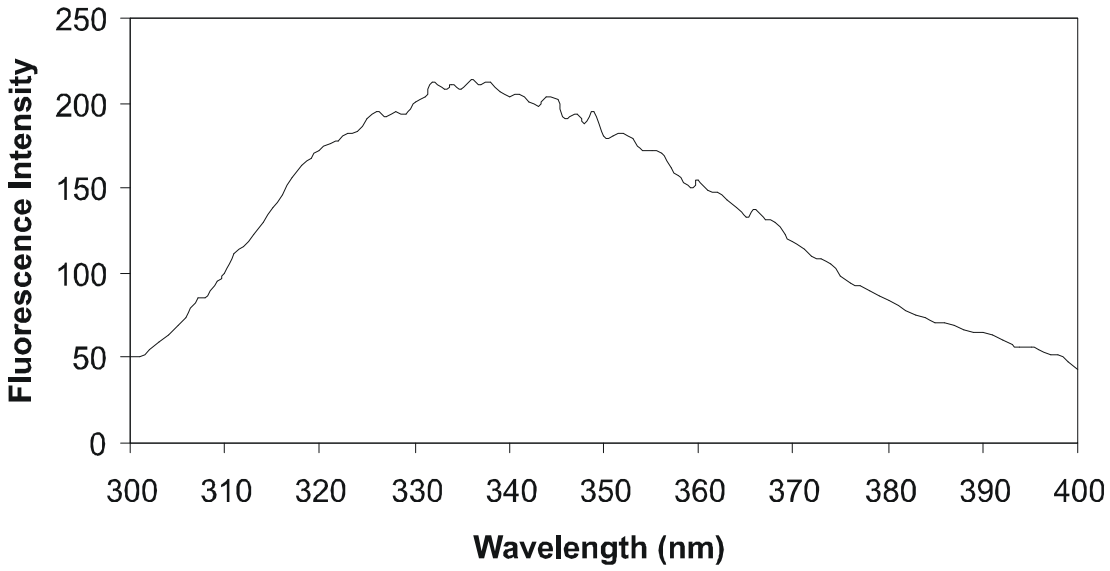
Fluorescence Intensity
250
200
150
100
50
0
300
310
320
330
340
350
360
370
380
390
400
Wavelength (nm)

**Figure 15**. Cartoon of hTRF1 substrates. Black lines represent random sequences used to anneal the substrates correctly

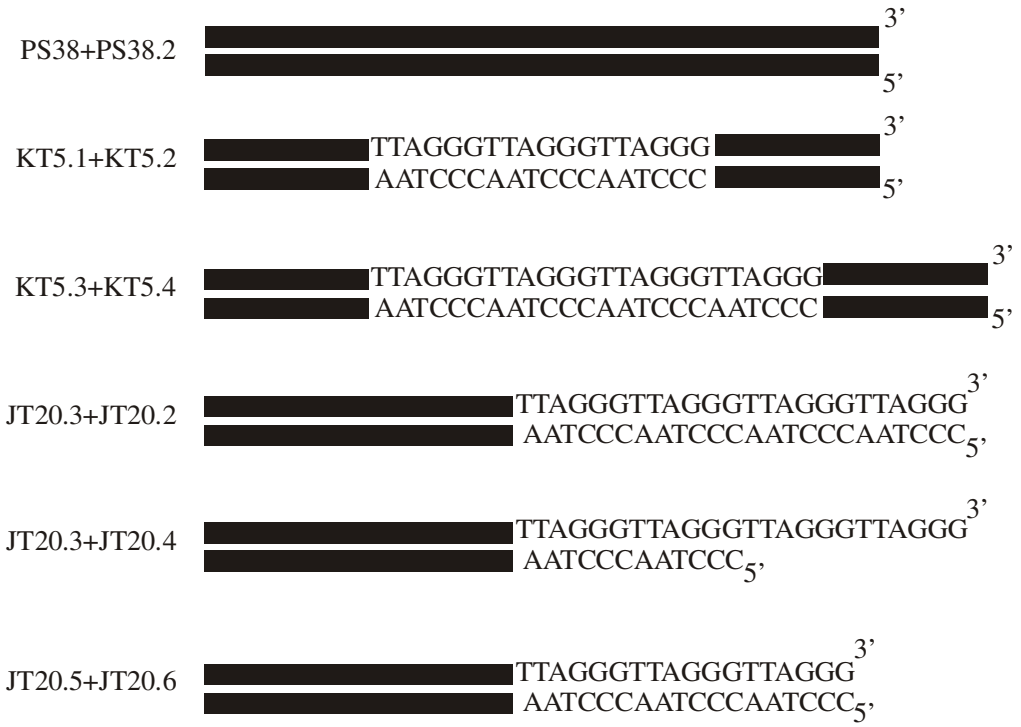
PS38+PS38.2
3'
5'
KT5.1+KT5.2
TTAGGGTTAGGGTTAGGG
AATCCCAATCCCAATCCC
3'
5'
KT5.3+KT5.4
TTAGGGTTAGGGTTAGGGTTAGGG
AATCCCAATCCCAATCCCAATCCC
3'
5'
JT20.3+JT20.2
TTAGGGTTAGGGTTAGGGTTAGGG
AATCCCAATCCCAATCCCAATCCC
3'
5'
JT20.3+JT20.4
TTAGGGTTAGGGTTAGGGTTAGGG
AATCCCAATCCC
3'
5'
JT20.5+JT20.6
TTAGGGTTAGGGTTAGGG
AATCCCAATCCCAATCCC
3'
5'

**Figure 16**. Equilibrium fluorescence quenching of hTRF1 by telomeric DNA and salt titration. Intrinsic fluorescence of hTRF1 is quenched only in the presence of telomeric DNA even in addition of excess salt (squares). The quenching effect of non-telomeric DNA (triangles) is not statistically different than that of buffer alone (circles).

.

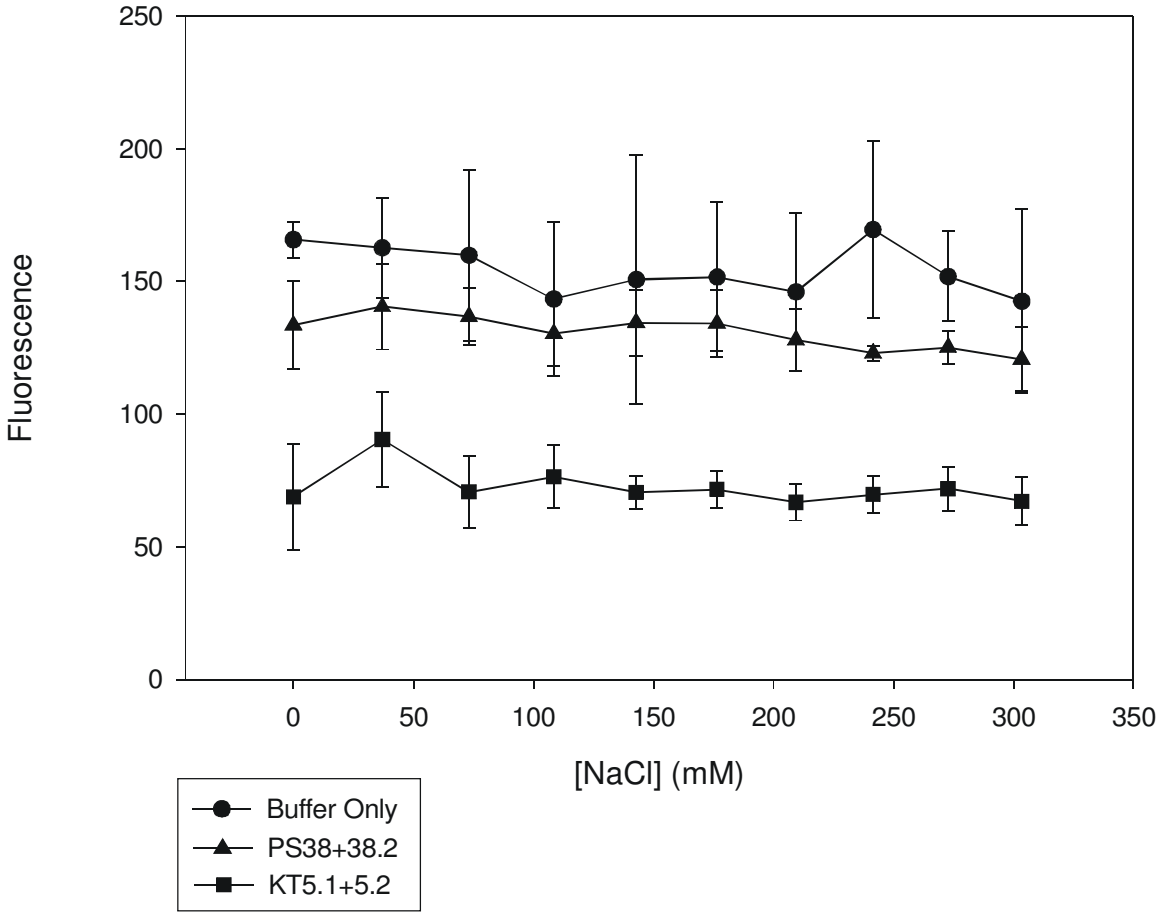
Fluorescence
250
200
150
100
50
0
0
50
100
150
200
250
300
350
[NaCl] (mM)
Buffer Only
PS38+38.2
KT5.1+5.2

**Figure 17**. Stopped flow intrinsic fluorescence measurements using hTRF1 in 10 second readings. a. hTRF1 fluorescence in the absence of DNA. b. hTRF1 fluorescence quenching upon the addition of DNA, regardless of sequence.

a.

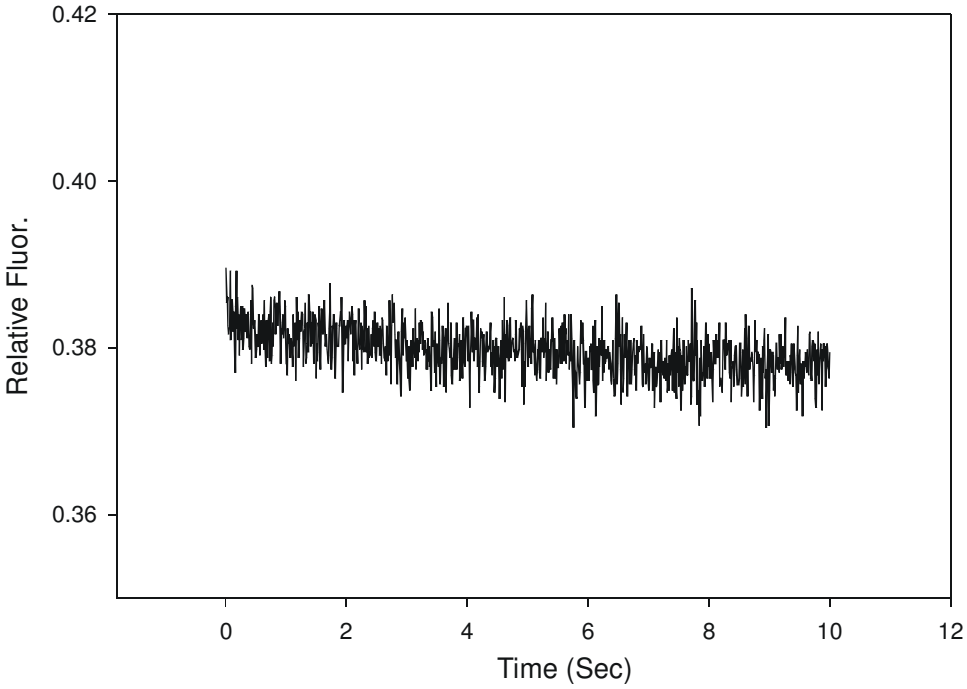
0.42
0.40
0.38
0.36
Relative Fluor.
0
2
4
6
8
10
12
Time (Sec)

b.

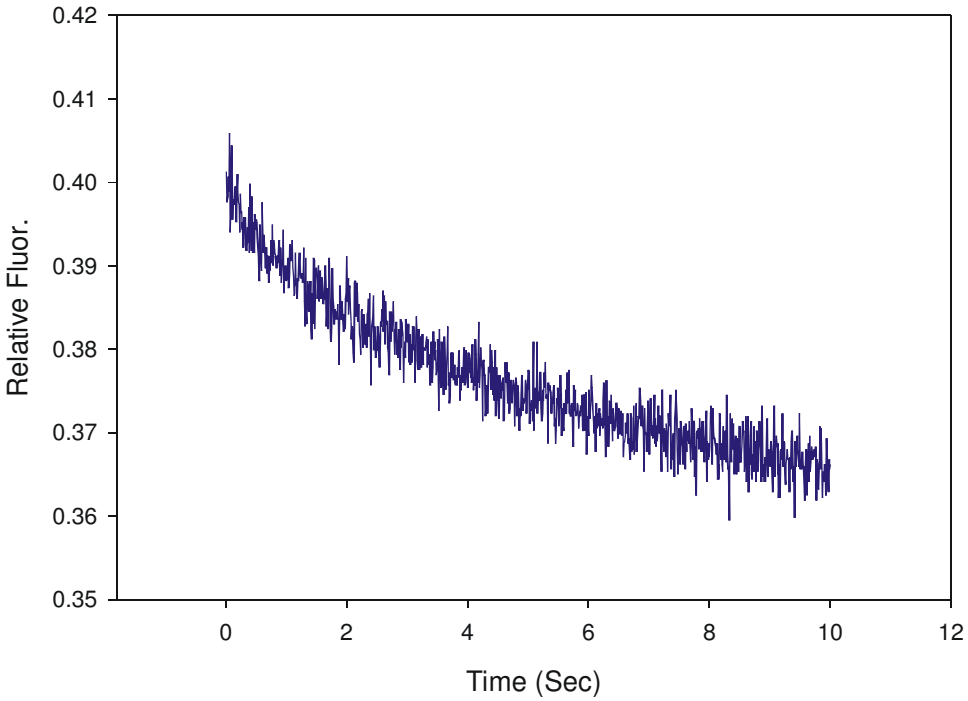
0.42
0.41
0.40
0.39
0.38
0.37
0.36
0.35
Relative Fluor.
0
2
4
6
8
10
12
Time (Sec)

**Figure 18**. Graph depicting the quenching of hTRF1's intrinsic fluorescence with non telomeric DNA (PS38+PS38.2). Top graph is a direct measurement of fluorescence quenching. The red line represents a single exponential decay curve. The bottom panel represents the fit of the curve to the fluorescence data by looking at the residual values around the curve.

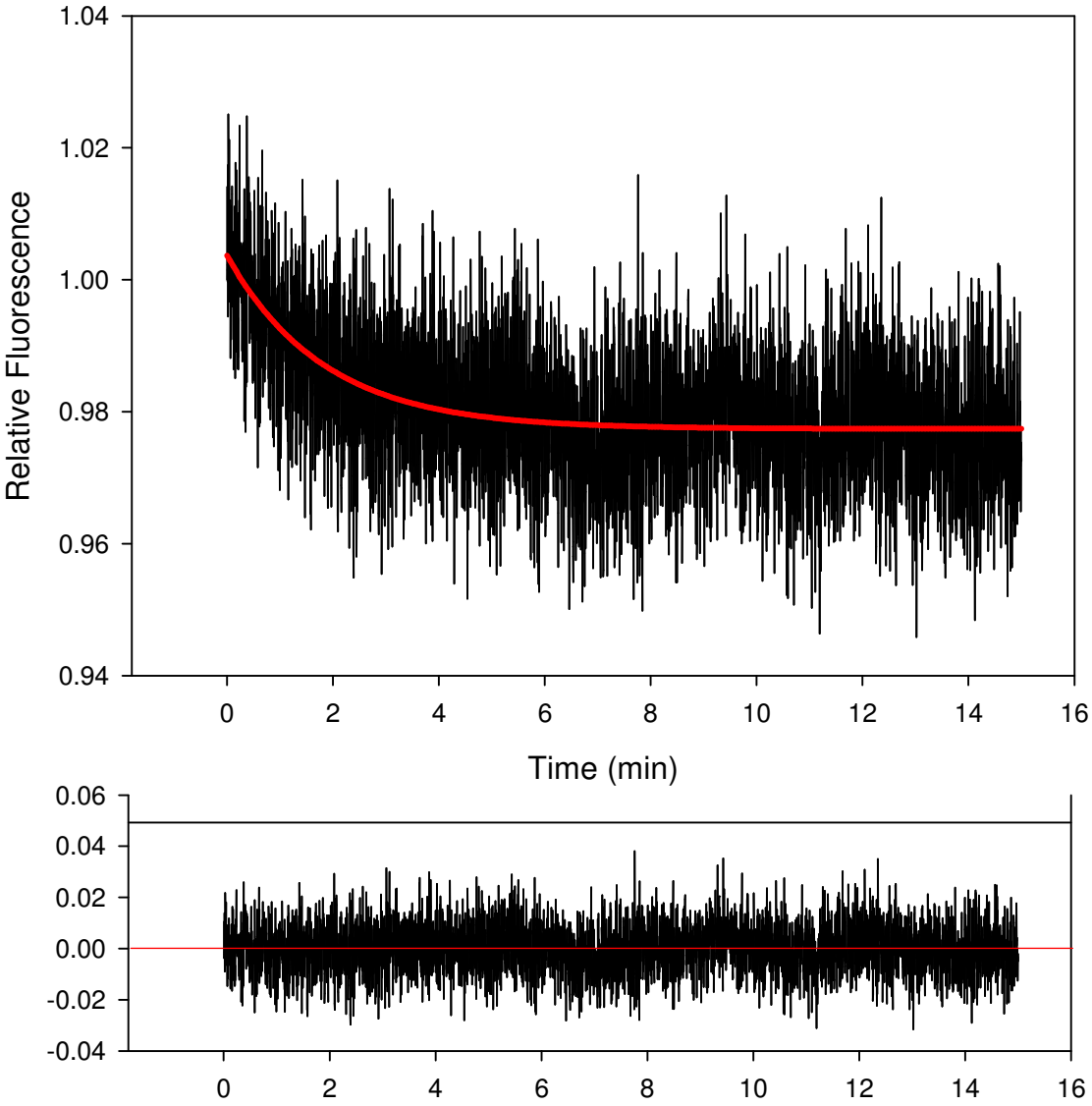
1.04
1.02
1.00
0.98
0.96
0.94
Relative Fluorescence
0
2
4
6
8
10
12
14
16
Time (min)
0.06
0.04
0.02
0.00
-0.02
-0.04
0
2
4
6
8
10
12
14
16

**Figure 19**. hTRF1 intrinsic fluorescence quenching by the substrate KT5.1+KT5.2 (3 internal repeats). The red line represents a single exponential decay curve and the green line represents a double exponential fit. The second panel represents the residuals from the single exponential curve (red line in top panel). The third panel depicts the residuals produced from the double exponential plot (green line in top panel).

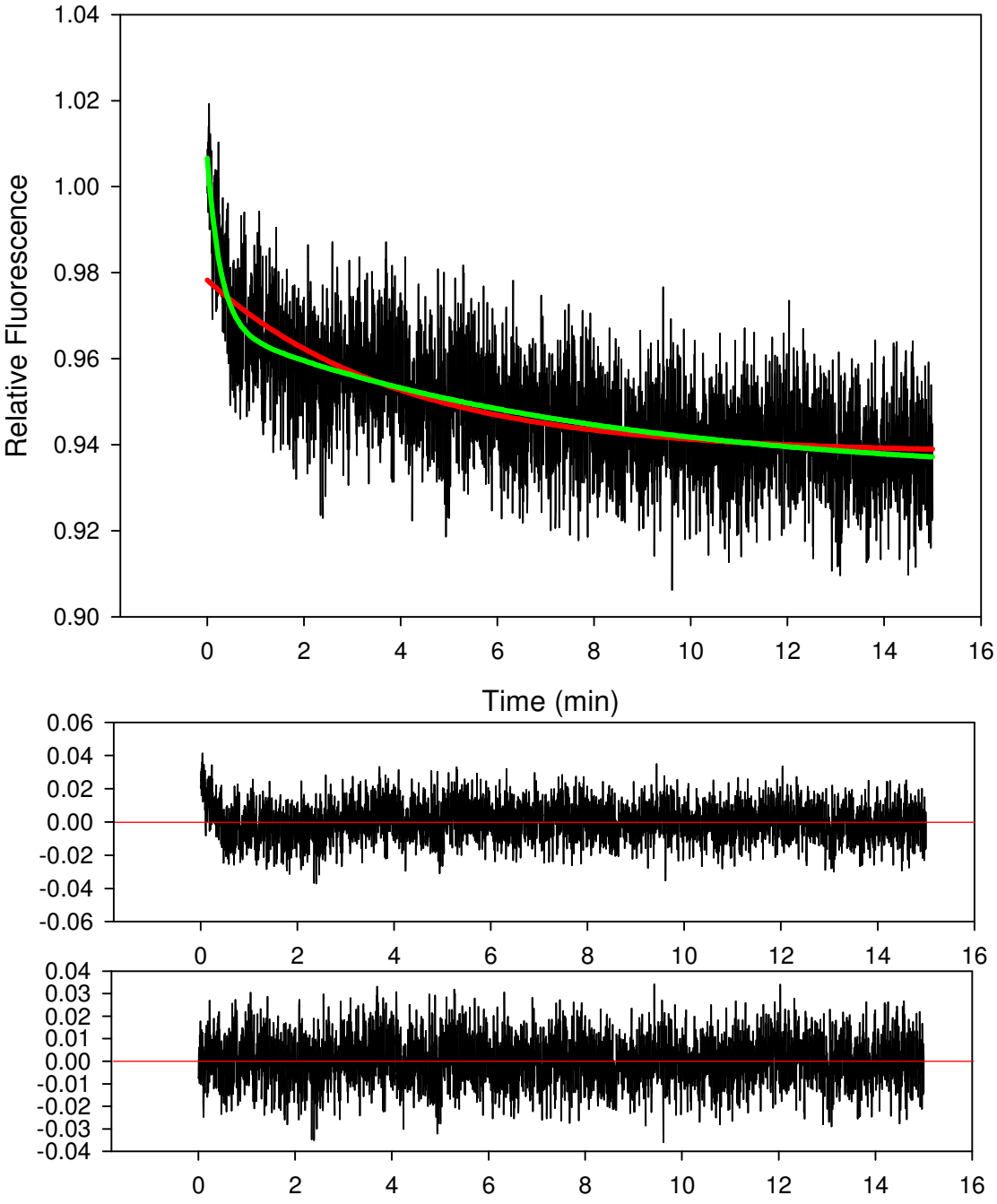
Relative Fluorescence
1.04
1.02
1.00
0.98
0.96
0.94
0.92
0.90
0
2
4
6
8
10
12
14
16
Time (min)
0.06
0.04
0.02
0.00
-0.02
-0.04
-0.06
0.04
0.03
0.02
0.01
0.00
-0.01
-0.02
-0.03
-0.04

**Figure 20**. Intrinsic fluorescence quenching for the KT5.3+KT5.4 (four internal repeats). In the top panel the red line for a single exponential decay is overlapped by the green line of a second exponential decay curve. Therefore, this data only fits a single exponential decay and since the residual values are also identical only one is shown here in the bottom panel.

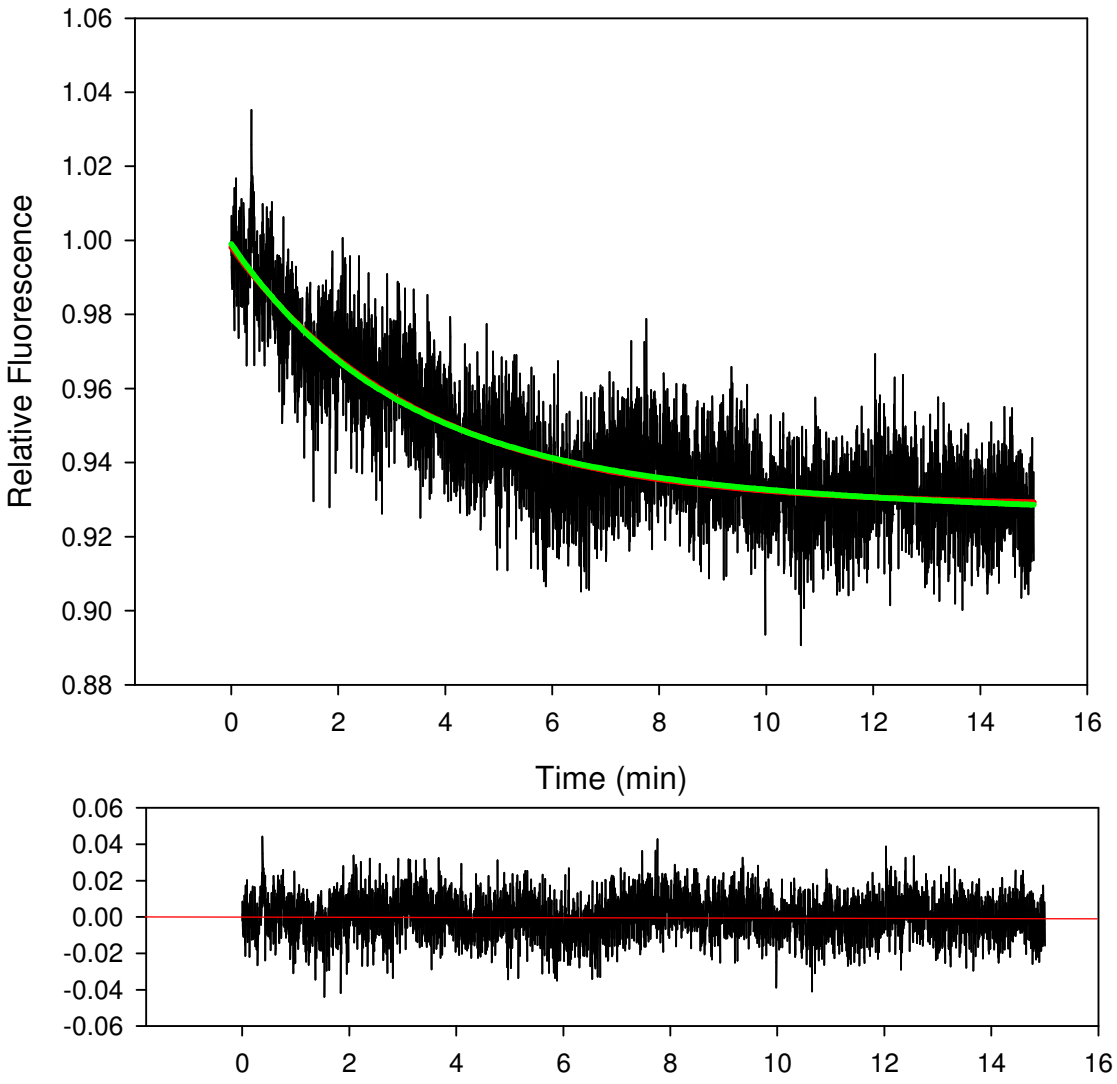
Relative Fluorescence
1.06
1.04
1.02
1.00
0.98
0.96
0.94
0.92
0.90
0.88
0
2
4
6
8
10
12
14
16
Time (min)
0.06
0.04
0.02
0.00
-0.02
-0.04
-0.06
0
2
4
6
8
10
12
14
16

**Figure 21**. Intrinsic fluorescence quenching for the JT20.2+JT20.3 substrate (four end repeats) and residual values as described for Figure 19.

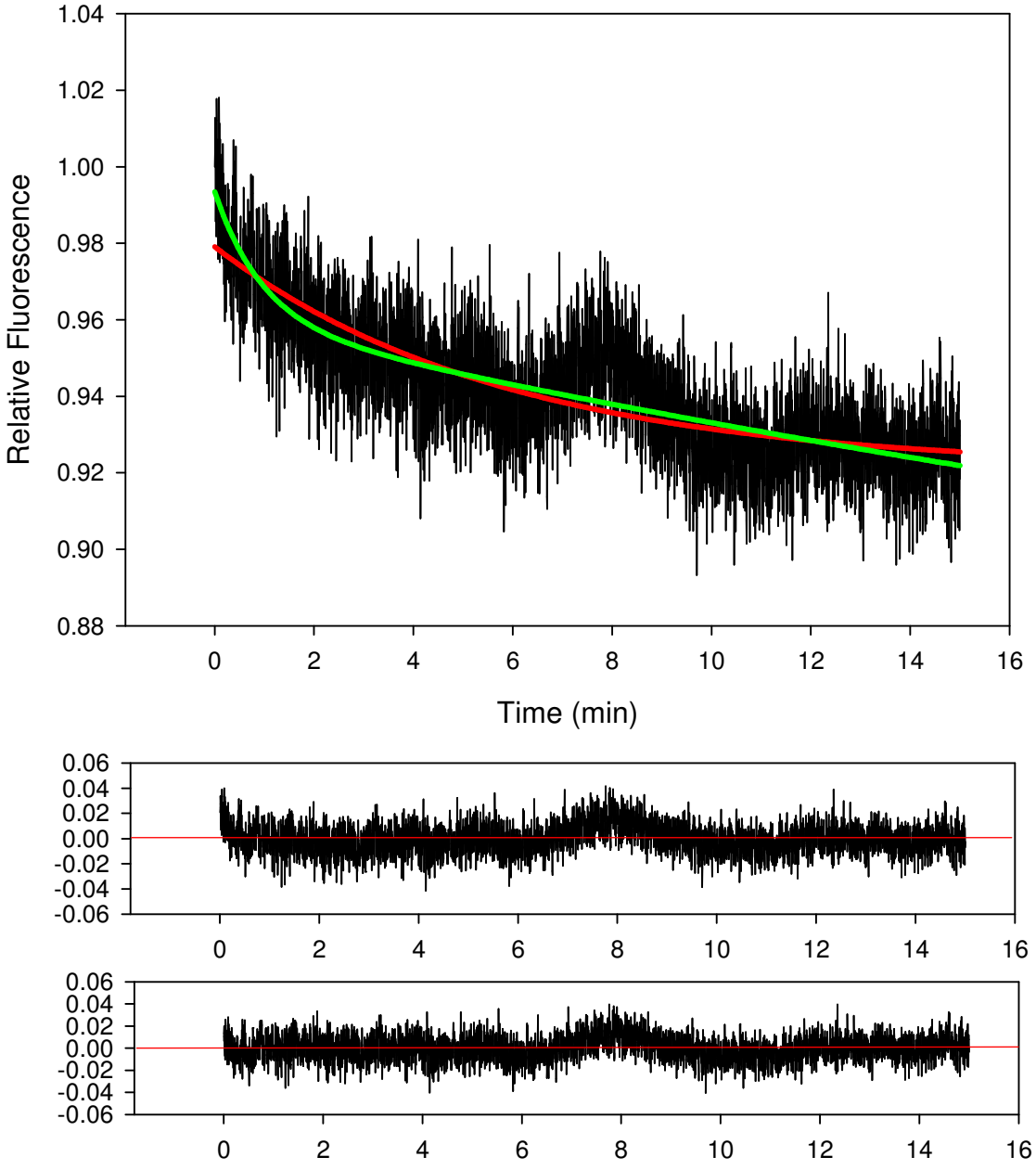
Relative Fluorescence
1.04
1.02
1.00
0.98
0.96
0.94
0.92
0.90
0.88
0
2
4
6
8
10
12
14
16
Time (min)
0.06
0.04
0.02
0.00
-0.02
-0.04
-0.06

**Figure 22**. Intrinsic fluorescence quenching for the JT20.4+JT20.3 substrate (2 double stranded end repeats with a double stranded overhang) and residuals as described in Figure 19.

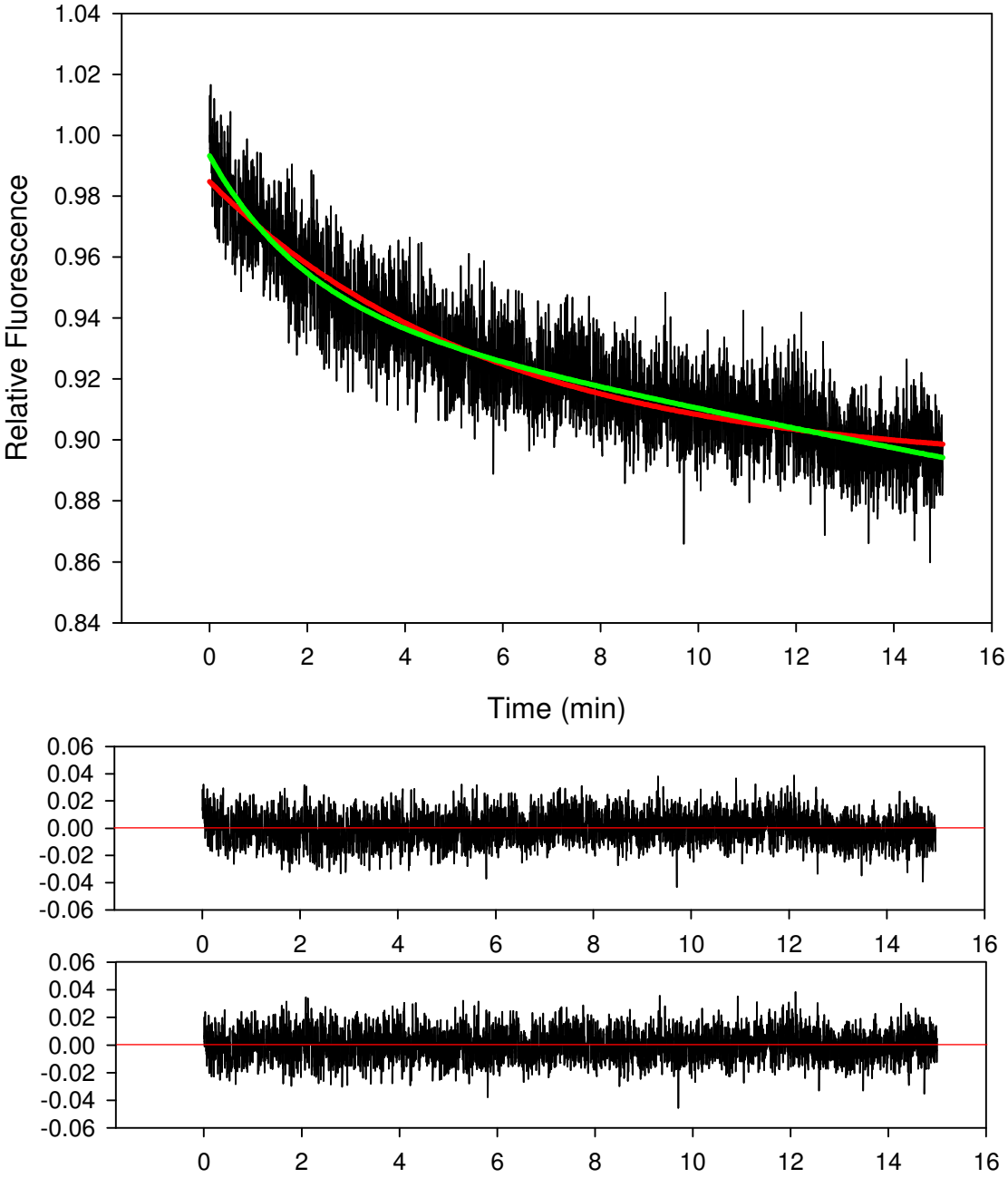
Relative Fluorescence
1.04
1.02
1.00
0.98
0.96
0.94
0.92
0.90
0.88
0.86
0.84
0
2
4
6
8
10
12
14
16
Time (min)
0.06
0.04
0.02
0.00
-0.02
-0.04
-0.06

**Figure 23**. Intrinsic fluorescence quenching for the JT20.5+JT20.6 substrate (three end repeats) and residuals as described in Figure 19.

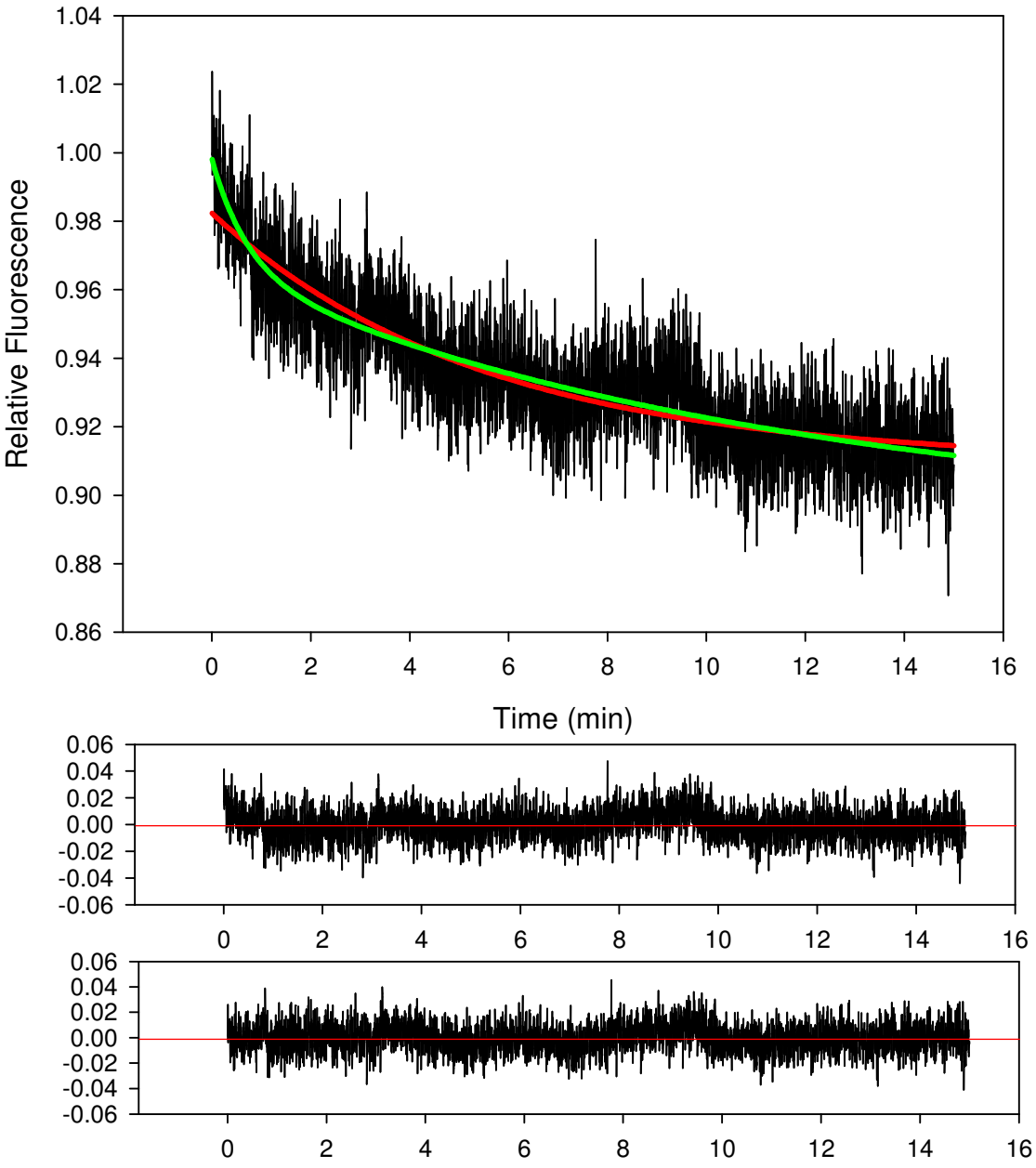
Relative Fluorescence
1.04
1.02
1.00
0.98
0.96
0.94
0.92
0.90
0.88
0.86
0
2
4
6
8
10
12
14
16
Time (min)
0.06
0.04
0.02
0.00
-0.02
-0.04
-0.06

**Figure 24**. Comparison of hTRF1 quenching between different substrates. In all graphs PS38+PS38.2 is present for reference. a. Comparison of all substrates with the telomeric repeats at the ends. b. Comparison of substrates with internal telomeric repeats. c. Comparison of substrates with three repeats. d. Comparison of substrates with four repeats.

a.

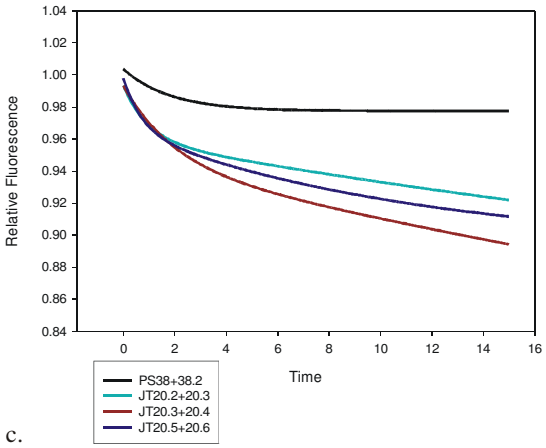
Relative Fluorescence
Time
PS38+38.2
JT20.2+20.3
JT20.3+20.4
JT20.5+20.6

b.

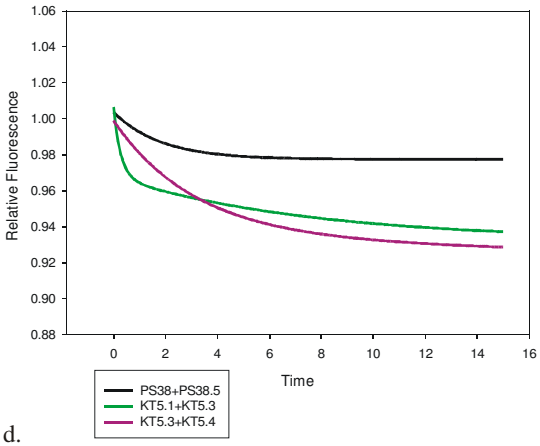
Relative Fluorescence
Time
PS38+PS38.5
KT5.1+KT5.3
KT5.3+KT5.4

c.

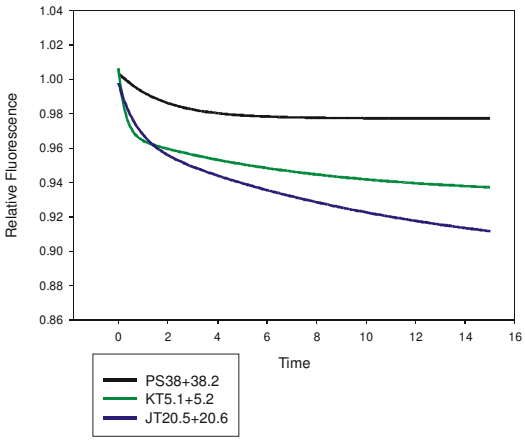
Relative Fluorescence
Time
PS38+38.2
KT5.1+5.2
JT20.5+20.6

d.

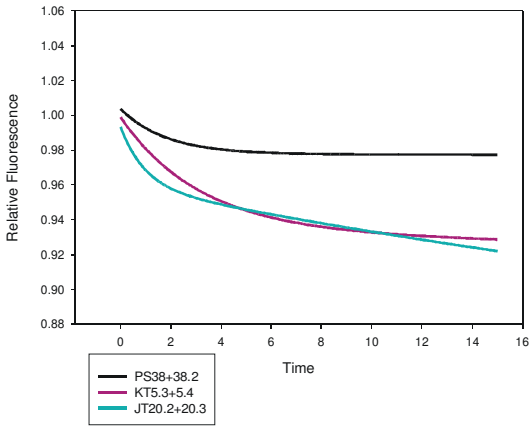
Relative Fluorescence
Time
PS38+38.2
KT5.3+5.4
JT20.2+20.3

# IV. DISCUSSION AND CONCLUSIONS

## hTEP1:

Here we report the first ever purification of full length hTEP1 (Figure 8). The fact that full length hTEP1 is so unstable in whole exptracts may account for why only small sub-domains were partially purified previously (Poderycki *et al.*, 2005). A significant advance was the addition of a precipitation step early in the purification, which was the 25% ammonium sulfate precipitation (Figure 7). At 25% ammonium sulfate, most other proteins do not precipitate, not only significantly purifying hTEP1 but more importantly separating it from the protein(s) that quickly degrade it. The next big hurdle that must be tackled is boosting the production of hTEP1, allowing the production of even more pure protein for future in-depth biochemical studies. We have partially overcome this limitation with a baculovirus expression system, however, there is still room for further progress in this area.

In this thesis, I have also demonstrated that full length hTEP1 binds hTR specifically (Figures 10 and 12). This interaction could not be competed with tRNA or whole yeast RNA. The interaction of hTEP1 with *in vitro* transcribed hTR can only be competed with the whole cell RNA of immortalized human cell line H1299 (Figure 11), which is most likely due to the presence of endogenous hTR. We also generated a random RNA molecule the same length as hTR. hTEP1 has some slight interaction with this molecule, but this interaction is easily competed away in the presence of competitor RNA (Figure 10). This specificity

for hTR *in vitro* would indicate that other segments of hTEP1 other than the p80 homology domain play a role in hTR binding. Another possible explanation could be that the hTEP1 in this work was produced in a eukaryotic system while the p80 homology domain was produced in *E. coli* (Poderycki *et al*., 2005). Therefore, we can not rule out post translational modifications as a reason why our protein binds hTR better *in vitro*.

Very recently Cohen et *al*., (2007) published the purification of catalytically active telomerase. In this study they used partial protein digests and mass spectroscopy to identify some of the protein components of telomerase and found that their protein only contained TERT and dyskerin. Though they did not find TEP1 as part of this complex, it can not be ruled out that hTEP1 still plays a critical role in telomere maintenance *in vivo*. For example, even though the *E. coli* polymerase III requires beta clamp for its function, during the purification the beta clamp may be lost depending on different salt conditions (Cull and McHenry, 1995). Therefore, though hTEP1 did not co-purify with the enzymatic activity of telomerase, there is no evidence that it does not play an important role in telomerase activity and telomere length maintenance. In fact, the evidence in this work that shows hTEP1 interacts with hTR specifically gives new importance to find what the exact role of hTEP1 is in telomere maintenance. Cohen et al., simply followed the activity of telomerase in G-strand synthesis. hTEP1 may play a role in C-strand synthesis, which our lab believes is carried out in concert with G-strand synthesis *in vivo*. The purification of this difficult protein puts us closer to reconstituting telomeric replication *in vitro*.

In conclusion, we have generated stable full length-hTEP1 which can bind its target (hTR) with specificity *in vitro*. Purifying full length hTEP1 will greatly enhance our ability to study the function of this protein and its greater role in telomeric maintenance. Since hTEP1 may be the bridge between hTERT and other possible proteins that create the telomerase complex, by being able to generate full length-functional hTEP1, we are one step closer to reconstituting the full (G and C strand synthesis) telomerase reaction *in vitro*.

hTRF1:

Here I have reported the first pre-steady state measurements of hTRF1 binding to DNA. The biggest surprise from these results was the discovery that hTRF1 binds non-telomeric DNA (Figures 17 and 18). The current dogma is that hTRF1 is a protein that only binds telomeric DNA. However, this picture is much more complicated. hTRF1 binds all DNA, however it has a higher affinity for telomeric DNA. This concept makes great sense since the Myb-like binding domain of hTRF1 is a DNA binding domain (reviewed in Lipsick 1996).

The second aspect of these experiments that was quite interesting was the fact that in the presence of telomeric DNA, the hTRF1's intrinsic fluorescence was quenched in a way that fit a double exponential decay (Figures 19, 21-23). This indicates that there are two separate events taking place. We predict that the first event is the DNA binding event. The second event is most likely due to a conformational change responsible for binding telomeric DNA specifically. This conclusion is drawn from our work and is supported by an additional line of research. Nashikawa *et al*. (2001) solved an NMR structure of the hTRF1 DNA

binding domain. In this study they discovered that an N-terminal arm of the binding domain becomes more ordered and interacts with the minor groove of the telomeric DNA. Our studies fit well with the information gathered from the NMR data.

One aspect of the fluorescence quenching that was puzzling was the presence of a spike in fluorescence around eight minutes that only occurred with half of the substrates (Figures 20, 21, and 23). This made curve fitting for the data of those substrates difficult. The exact reason for this spike is unknown. One could argue that this spike was a result of more than one protein interacting with the DNA, especially in cases where there were four telomeric repeats, however, in one case the spike occurred in the presence of three repeats. However, in studies where only the DNA binding domain of hTRF1 was used, only two telomeric repeats were required (Nashikawa *et al*., 2001; König *et al.,* 1998), and three repeats were the minimum needed when using full length hTRF1 (Zhong *et al*., 1992; Bianchi *et al*., 1997). Further experiments are necessary with a wider range of substrates to determine the exact nature and the relevance of this spike.

Through this study we have made a significant progress in understanding how hTRF1 works. Our model indicates that hTRF1 binds DNA, and scans it for telomeric tracts. Upon reaching the telomeric tract, hTRF1 slowly changes confirmation and binds the telomeric DNA more stably (Figure 25). This model fits very well with the role hTRF1 plays in the cell as a protein that binds and stabilizes telomeric DNA.

**Figure 25**. Cartoon of the possible hTRF1 mechanism. a. The blue ribbon represent random DNA sequences. The hTRF1 homodimer is able to bind this DNA but only weakly and can easily fall off. b. The red ribbon represents a stretch of telomeric DNA. The hTRF1 homodimer goes through a conformational change upon interacting with the telomeric DNA, allowing it to bind tightly.

a.

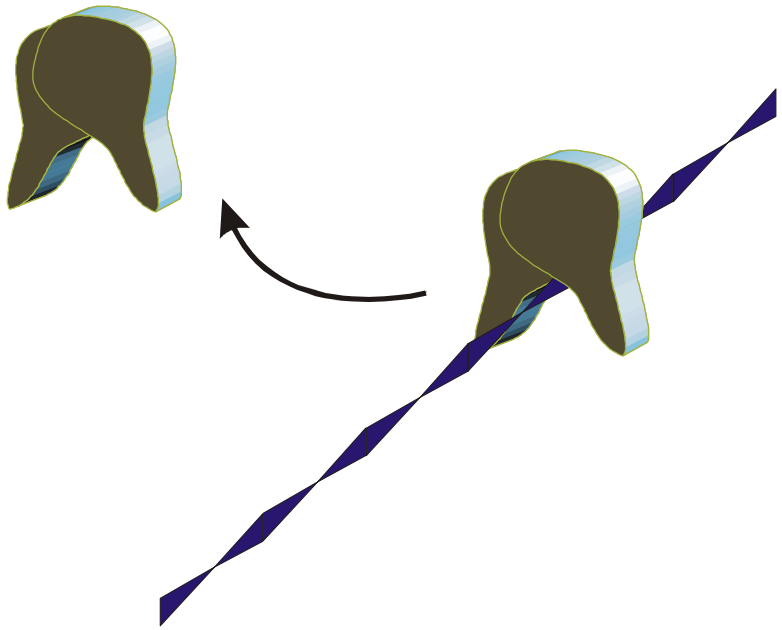

b.

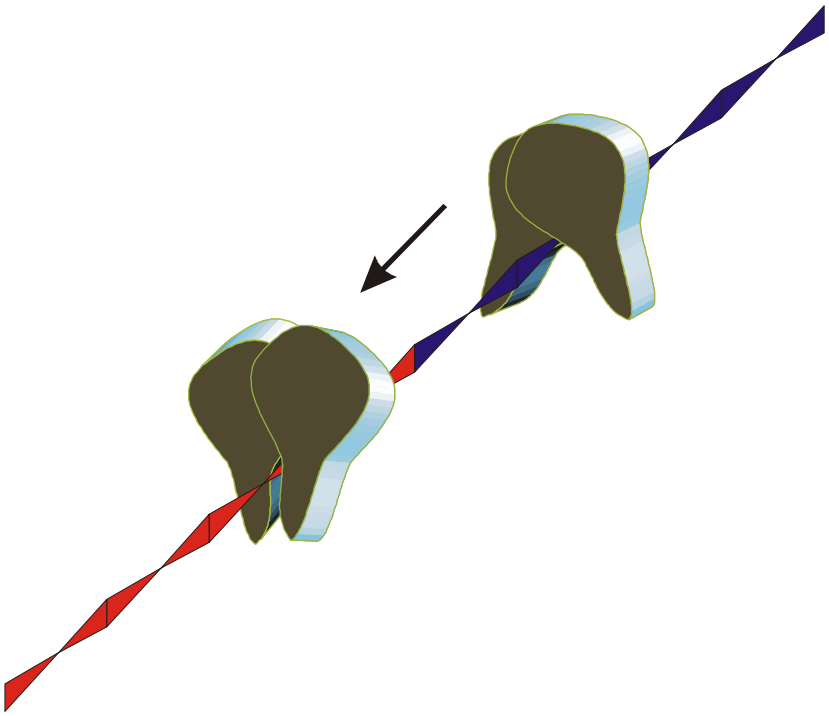

## V. BIBLIOGRAPHY


Arai, K., Masutomi, K., Khurts, S., Kaneko, S., Kobayashi, K., and Murakami, S. (2002) Two independent regions of human telomerase reverse transcriptase are important for its oligomerization and telomerase activity. *J. Biol. Chem.* 277:8538-8544.

Bachand, F., and Autexier, C. (2001) Functional regions of human telomerase reverse transcriptase and human telomerase RNA required for telomerase activity and RNA-protein interactions. *Mol. Cell. Biol*. 21:1888-1897.

Bianchi, A., Smith, S., Chong, L., Elias, P., and de Lange, T. (1997) TRF1 is a dimer and bends telomeric DNA. *EMBO J.*16:1785-1794.

Blackburn, E.H., and Gall, J.G. (1978) A tandemly repeated sequence at the termini of the extrachromosomal ribosomal RNA genes in *Tetrahymena*. *J. Mol. Biol*. 120:33-53.

Blackburn, E.H., and Szostak, J.W. (1984) The molecular structure of centromeres and telomeres. *Ann. Rev. Biochem*. 53:163-194.

Blasco, M.A., Lee, H., Hande, M.P., Samper, E., Lansdorp, P.M., DePinho, R.A., and Greider, C.W. (1997) Telomere shortening and tumor formation by mouse cells lacking telomerase RNA. *Cell* 91:25-34.

Bodnar, A.G., Ouellette, M., Frolkis, M., Holt, S.E., Chiu, C., Morin, G.B., Harley, C.B., Shay, J.W., Lichtsteiner, S., and Wright, W.E. (1998) Extension of life-span by introduction of telomerase into normal human cells. *Science* 279:349-352.

Broccoli, D., Smogorzewska, A., Chong, L., and de Lange, T. (1997) Human telomeres contain two distinct Myb-related proteins, TRF1 and TRF2. *Nat. Genet*. 17:231-235.

Chen, J.L., Blasco, M.A., and Greider, C.W. (2000) Secondary structure of vertebrate telomerase RNA. *Cell* 100:503-514.

Chen, J.L., and Greider, C.W. (2003) Determinants in mammalian telomerase RNA that mediate enzyme processivity and cross-species incompatibility. *EMBO J.* 22:304-314.

Chong, L., van Steensel, B., Broccoli, D., Erdjument-Bromage, H., Hanish, J., Tempst, P., and de Lange T. (1995) A human telomeric protein. *Science* 270:1663-1667.

Cohen, S.B., Graham, M.E., Lovrecz, G.O., Bache, N., Robinson, P.J., and Reddel, R.R. (2007) Protein composition of catalytically active human telomerase from immortal cells. *Science* 315:1850-1853.

Counter, C.M., Avilion, A.A., LeFeuvre, C.E., Stewart, N.G., Greider, C.W., Harley, C.B., and Bacchetti, S. (1992) Telomere shortening associated with chromosome instability is arrested in immortal cells which express telomerase activity. *EMBO J.* 11:1921-1929.

Counter, C.M., Hahn, W.C., Wei, W.Y., Caddle, S.D., Beijersbergen, R.L., Lansdorp, P.M., Sedivy, J.M., Weinberg, R.A. (1998a) Dissociation among in vitro telomerase activity, telomere maintenance, and cellular immortalization. *Proc. Natl. Acad. Sci.* 95:14723-14728.

Counter, C.M., Hahn, W.C., Wei, W., Dickinson Caddle, S., Beijersbergen, R.L., Lansdorp, P.M., Sedivy, J.M., and Weinberg, R.A. (1998b) Dissociation among in vitro telomerase activity, telomere maintenance, and cellular immortalization. *Proc. Natl. Acad. Sci.* 95:14723-14728.

Cull, M.G., and McHenry, C.S. (1995) Purification of *Escherichia coli* DNA polymerase III holoenzyme. *Methods Enzymol*. 262:22-35

Dandjinou, A.T., Dionne, I., Gravel, S., LeBel, C., Parenteau, J., and Wellinger, R.J. (1999) Cytological and functional aspects of telomere maintenance. [Review] *Histol. Histopathol*. 14:517-524.

Dionne, I., and Wellinger, R.J. (1996) Cell cycle-regulated generation of single-stranded G-rich DNA in the absence of telomerase. *Proc. Natl. Acad. Sci*. 93:13902-13907.

Feng, J., Funk, W.D., Wang, S.S., Weinrich, S.L., Avilion, A.A., Chiu, C.P., Adams, R.R., Chang, E., Allsopp, R.C., Yu, J., Le, S., West, M.D., Harley, C.B., Andrews, W.H., Greider, C.W., and Villeponteau, B. (1995) The RNA component of human telomerase. *Science* 269:1236-1241.

Greider, C.W., and Blackburn, E.H. (1985) Identification of a specific telomere terminal transferase activity in tetrahymena extracts. *Cell* 43:405-413.

Greider, C.W. (1996) Telomere length regulation. *Annu. Rev. Biochem*. 63:337-365.

Griffith, J.D., Comeau, L., Rosenfield, S., Stansel, R.M., Bianchi, A., Moss, H., and de Lange, T. (1999) Mammalian telomeres end in a large duplex loop. *Cell* 97:503-514.

Harley, C.B., Futcher, A.B., and Greider, C.W. (1990) Telomeres shorten during aging of human fibroblasts. *Nature* 345:458-460.

Harrington, L., McPhail, T., Mar, V., Zhou, W., Oulton, R., Amgen EST Program, Bass, M.B., Arruda, I., and Robinson, M.O. (1997) A mammalian telomerase-associated protein. *Science* 275:973-977.

Hastie, N.D., Dempster, M., Dunlop, M.G., Thompson, A.M., Green, D.K., and Allshire, R.C. (1990) Telomere reduction in human colorectal carcinoma and with aging. *Nature* 346:866-868.

Hemann, M.T., and Greider, C.W. (1999) G-strand overhangs on telomeres in telomerase-deficient mouse cells. *Nucleic Acids Res.* 27:3964-3969.

Henderson, E., Hardin, C.C., Walk, S.K., Tinoco, Jr., I., and Blackburn, E.H. (1987) Telomeric DNA oligonucleotides form novel intramolecular structures containing guanine-guanine base pairs. *Cell* 51:899-908.

Holt, S.E., and Shay, J.W. (1999) Role of telomerase in cellular proliferation and cancer. [Review] *J. Cell. Physiol*. 180:10-18.

Hom, L.G., and Wolkman, L.E. (1998) Preventing proteolytic artifacts in the baculovirus expression system. *BioTechniques* 25:18-20.

Huffman, K.E., Levene, S.D., Tesmer, V.M., Shay, J.W., and Wright, W.E. (2000) Telomere shortening is proportional to the size of the G-rich telomeric 3'-overhang. *J. Biol. Chem.* 275:19719-19722.

Karlseder, J., Broccoli, D., Dai, Y., Hardy, S., and de Lange, T. (1999) p53- and ATM-dependent apoptosis induced by telomeres lacking TRF2. *Science* 283:1321-1325.

Karlseder, J., Smogorzewska, A., and de Lange, T. (2002) Senescence induced by altered telomere state, not telomere loss. *Science* 295:2446-2449.

Kickhoefer, V.A., Stephen, A.G., Harrington, L., Robinson, M.O., and Rome, L.H. (1999) Vaults and telomerase share a common subunit, TEP1. *J. Biol. Chem.* 274:32712-32717.

Kim, N.W., Piatyszek, M.A., Prowse, K.R., Harley, C.B., West, M.D., Ho, P.L.C., Coviello, G.M., Wright, W.E., Weinrich, S.L., and Shay, J.W. (1994)

Specific association of human telomerase activity with immortal cells and cancer. *Science* 266:2011-2015.

König, P., Fairall, L., and Rhodes, D. (1998) Sequence-specific DNA recognition by the Myb-like domain of the human telomere binding protein TRF1: a model for the protein-DNA complex. *Nucleic. Acids Res*. 26:1731-1740.

Krutilina, R.I., Oei, S., Buchlow, G., Yau, P.M., Zalensky, A.O., Zalenskaya, I.A., Bradbury, E.M., and Tomilin, N.V. (2001) A negative regulator of telomere-length protein TRF1 is associated with interstitial (TTAGGG)n blocks in immortal Chinese hamster ovary cells. *Biochem. Biophys. Res. Commun*. 280:471-475.

Ku, W.C., Cheng, A.J. and Wang, T.C.V. (1997) Inhibition of telomerase activity by PKC inhibitors in human nasopharyngeal cancer cells in culture. *Biochem. Biophys. Res. Commun*. 241:730-736.

Li, H., Zhao, L., Funder, J.W., and Liu, J.P. (1997) Protein phosphatase 2A inhibits nuclear telomerase activity in human breast cancer cells. *J. Biol. Chem.* 272:16729-16732.

Li, H., Zhao, L., Yang, Z., Funder, J.W., and Liu, J.P. (1998) Telomerase is controlled by protein kinase cα in human breast cancer cells. *J. Biol. Chem.* 273:33436-33442.

Lipsick, J.S. (1996) One billion years of Myb. *Oncogene* 13:223–235.

Liu, Y., Snow, B.E., Hande, M.P., Baerlocher, G., Kickhoefer, V.A., Yeung, D., Wakeham, A., Itie, A., Siderovski, D.P., Lansdorp, P.M., Robinson, M.O., and Harrington, L. (2000) Telomerase-associated protein TEP1 is not essential for telomerase activity or telomere length maintenance in vivo. *Mol. Cell. Biol*. 20:8178-8184.

Loayza, D., and de Lange, T. (2003) POT1 as a terminal transducer of TRF1 telomere length control. *Nature* 423:1013-1018.

Lundberg, A.S., Hahn, W.C., Gupta, P., and Weinberg, R.A. (2000) Genes involved in senescence and immortalization. [Review] *Curr. Opin. Cell Biol.* 12:705-709.

Makarov, V.L., Hirose, Y., and Langmore, J.P. (1997) Long G tails at both ends of human chromosomes suggest a C strand degradation mechanism for telomere shortening. *Cell* 88:657-666

Martensen, P.M., and Justesen, J. (2001) Specific inhibitors prevent proteolytic degradation of recombinant proteins expressed in High Five™ cells. *BioTechniques* 30:782-791.

Masutomi, K., Kaneko, S., Hayashi, N., Yamashita, T., Shirota, Y., Kobayashi, K., and Murakami, S. (2000) Telomerase activity reconstituted *in vitro* with purified human telomerase reverse transcriptase and human telomerase RNA component. *J. Biol. Chem.* 275:22568-22573.

McClintock, B. (1939) The behavior in successive nuclear divisions of a chromosome broken at meiosis. *Genetics* 25:405-416.

McClintock, B. (1940) The stability of broken ends of chromosomes in zea mays. *Genetics* 26:234-282.

McClintock, B. (1942) The fusion of broken ends of chromosomes following nuclear fusion. *Proc. Natl. Acad. Sci*. 28:458-463.

McElligott, R., and Wellinger, R.J. (1997) The terminal DNA structure of mammalian chromosomes. *EMBO J*. 16:3705-3714.

Meyerson, M., Counter, C.M., Eaton, E.N., Ellisen, L.W., Steiner, P., Dickinson Caddle, S., Ziaugra, L., Beijersbergen, R.L., Davidoff, M.J., Liu, Q., Bacchetti, S., Haber, D.A., Weinberg, R.A. (1997) hEST2, the putative human telomerase catalytic subunit gene, is up-regulated in tumor cells and during immortalization. *Cell* 90:785-795.

Morin, G.B. (1989) The human telomere terminal transferase enzyme is a ribonucleoprotein that synthesizes TTAGGG repeats. *Cell* 59:521-529.

Moyzis, R.K., Buckingham, J.M., Cram, L.S., Dani, M., Deaven, L.L., Jones, M.D., Meyne, J., Ratliff, R.L., and Wu, J.R. (1988) A highly conserved repetitive DNA sequence, (TTAGGG)n, present at the telomeres of human chromosomes*. Proc. Natl. Acad. Sci*. 85:6622-6626.

Muller, H.J. (1938) The remaking of chromosomes. *Coll. Net.* 13:181-198.

Muñoz-Jordán, J.L., Cross, G.A.M., de Lange, T., Griffith J.D. (2001) T-loops at trypanosome telomeres. *EMBO J.* 20:579-588.

Nakamura, T.M., Morin, G.B., Chapman, K.B., Weinrich, S.L., Andrews, W.H., Lingner, J., Harley, C.B., and Cech, T.R. (1997) Telomerase catalytic subunit homologs from fission yeast and human. *Science* 277:955-959.

Neer, E.J., Schmidt, C.J., Nambudripdad, R., and Smith, T.F. (1994) The ancient regulatory-protein family of WD-repeat proteins. *Nature* 371:297-300.

Nishikawa, T., Okamura, H., Nagadoi, A., König, P., Rhodes, D., and Nishimura, Y. (2001) Solution structure of a telomeric DNA complex of human TRF1. *Structur*e 9:1237-1251.

Nozawa, K., Suzuki, M., Takemura, M., and Yoshida, S. (2000) *In vitro* expansion of mammalian telomere repeats by DNA polymerase α-primase. *Nucleic. Acids Res.* 28:3117-3124.

Ohki, R., Tsurimoto, T., and Ishikawa, F. (2001) *In vitro* reconstitution of the end replication problem. *Mol. Cell. Biol*. 21: 5753-5766.

Olovnikov, A.M. (1971) Principle of Marginotomy in the synthesis of polynucleotides at a template. *Doklady Biochem.* 201:394-397.

Ouellette, M.M., Aisner, D.L., Savre-Train, I., Wright, W.E., and Shay, J.W. (1999) Telomerase activity does not always imply telomere maintenance. *Biochem. Biophys. Res. Commun*. 254:795-803.

Pays, E., Laurent, M., Delinte, K., Van Meirvenne, N., and Steinert, M. (1983) Differential size variations between transcriptionally active and inactive telomeres of *Trypanosoma*. *Nucleic. Acids Res.* 11:8137-8146.

Phan, A.T., and Mergny, J.L. (2002) Human telomeric DNA: G-quadruplex, i-motif and Watson-Crick double helix. *Nucleic. Acids Res.* 30:4618-4625.

Pderycki, M.J., Rome, L.H., Harrington, L., and Kickhoefer, V.A. (2005) The p80 homology region of TEP1 is sufficient for its association with the telomerse and vault RNAs, and the vault particle. *Nucleic Acids Res*. 33:892-902.

Reveal, P.M., Henkels, K.M., and Turchi, J.J. (1997) Synthesis of the mammalian telomere lagging strand in vitro. *J. Biol. Chem*. 272:11678-11681.

Rudolph, K.L., Chang, S., Lee, H., Blasco, M., Gottlieb, G.J., Greider, C., and DePinho, R.A. (1999) Longevity, stress response, and cancer in aging telomerase-deficient mice. *Cell* 96:701-712.

Smith, S., and de Lange, T. (1997) TRF1, a mammalian telomeric protein. [Review] *Trends. Genet*. 13:21-26.

Smogorzewska, A., van Steensel, B., Bianchi, L., Oelmann, S., Schaefer, M.R., Schnapp, G., and de Lange, T. (2000) Control of human telomere length by TRF1 and TRF2. *Mol. Cell. Biol.* 20:1659-1668.

Smogorzewska, A., and de Lange, T. (2002) Different telomere damage signaling pathways in human and mouse cells. *EMBO J*. 21:4338-4348.

Smucker, E.J., and Turchi, J.J. (2001) TRF1 inhibits telomere c-strand DNA synthesis in vitro. *Biochemistry* 40:2426-2432.

Stansel, R.M., de Lange, T., and Griffith, J.D. (2001) T-loop assembly in vitro involves binding of TRF2 near the 3' telomeric overhang. *EMBO J*. 20:5532-5540.

van Steensel, B., and de Lange, T. (1997) Control of telomere length by the human telomeric protein TRF1. *Nature* 385:740-743.

van Steensel, B., Smogorzewska, A., and de Lange, T. (1998) TRF2 protects human telomeres in vitro. *Cell* 92:401-413.

Vaziri, H., West, M.D., Allsopp, R.C., Davison, T.S., Wu, Y., Arrowsmith, C.H., Poirier, G.G., and Benchimol, S. (1997) ATM-dependent telomere loss in aging human diploid fibroblasts and DNA damage lead to the post-translational activation of p53 protein involving poly(ADP-ribose) polymerase. *EMBO J*. 16:6018-6033.

Vaziri, H., and Benchimol, S. (1999) Alternative pathways for the extension of cellular life span: inactivation of p53/pRb and expression of telomerase. *Oncogene* 18:7676-7680.

Vulliamy, T., Marrone, A., Goldman, F., Dearlove, A., Bessler, M., Mason, P.J., and Dokal, I. (2001) The RNA component of telomerase is mutated in autosomal dominant dyskeratosis congenita. *Nature* 413:432-435.

Watson, J.D., and Crick, F.H.C. (1953) Genetical implications of the structure of deoxyribonucleic acid. *Nature* 171:984-967.

Watson, J.D. (1972) Origin of Concatemeric T7 DNA. *Nature New Biol*. 239:197-201.

Wellinger, R.J., Ethier, K., Labrecque, P., and Zakian, V.A. (1996) Evidence for a new step in telomere maintenance. *Cell* 85:426-433.

Williamson, J.R., Raghuraman, M.K., and Ceck, T.R. (1989) Monovalent cation-induced structure of telomeric DNA: the G-quartet model. *Cell* 59:871-880.

Wright, W.E., Tesmer, V.M., Huffman, K.E., Levene, S.D., and Shay, J.W. (1997) Normal human chromosomes have long G-rich telomeric overhangs at one end. *Genes Dev.* 11:2801-2809.

Zhang, X., Mar, V., Zhou, W., Harrington, L., and Robinson, M.O. (1999) Telomere shortening and apoptosis in telomerase-inhibited human tumor cells. *Genes Dev.* 13:2388-2399.

Zhong, Z., Shiue, L., Kaplan, S., and de Lange, T. (1992) A mammalian factor that binds telomeric TTAGGG repeats in vitro. *Mol. Cell. Biol.* 12:4834-4843.